A fossiliferous spherule-rich bed at the Cretaceous–Paleogene (K–Pg) boundary in Mississippi, USA: implications for the K–Pg mass extinction event in the Mississippi Embayment and Eastern Gulf Coastal Plain

James D. Witts[1], Neil H. Landman[1], Matthew P. Garb[2], Caitlin Boas[2], Ekaterina Larina[3], Remy Rovelli[4], Lucy E. Edwards[5], Robert M. Sherrell[6,7], and J. Kirk Cochran[8]

[1]*Division of Paleontology (Invertebrates), American Museum of Natural History, New York, NY 10024, USA*

[2]*Department of Earth and Environmental Sciences, Brooklyn College, Brooklyn, NY 11210, USA*

[3]*University of Southern California, Department of Earth Sciences, Los Angeles, CA 90018, USA*

[4]*Department of Earth and Planetary Sciences, The University of New Mexico, Albuquerque, NM 87131, USA*

[5]*U.S. Geological Survey, Mail Stop 926A, Reston, VA 20192, USA*

[6]*Department of Marine and Coastal Sciences, Rutgers University, Piscataway, NJ 08901, USA*

[7] *Department of Earth and Planetary Sciences, Rutgers University, Piscataway, NJ 08901, USA*

[8]*School of Marine and Atmospheric Science, Stony Brook University, Stony Brook, NY 11794, USA*

[The final, fully formatted version of this article is available online at Cretaceous Research: https://doi.org/10.1016/j.cretres.2018.06.002]

Abstract

We describe an outcrop of the Cretaceous–Paleogene (K–Pg) boundary exposed due to construction near New Albany, Union County, Mississippi. It consists of the Owl Creek Formation and overlying Clayton Formation. The Owl Creek Formation is rich in the ammonites *Discoscaphites iris* and *Eubaculites carinatus*, which, along with biostratigraphically important dinoflagellate cysts and calcareous nannofossils, indicate deposition occurred within the last 1 million years, most likely last 500 kyrs, of the Cretaceous. The base of the overlying Clayton Formation marks the K–Pg boundary, and consists of a 15-30 cm thick muddy, poorly sorted quartz sand containing abundant spherules representing ejecta derived from the Chicxulub impact event. Impact spherules range in size from 0.5 mm to 1 mm in diameter and are hollow and well preserved, with details such as smaller vesicular spherules enclosed within. The spherules are altered to clay minerals such as smectite and are typical of those found at K–Pg boundary sites in the Gulf of Mexico and beyond. Spherules are scattered throughout the bed, and surface counts suggest an average of 4 spherules per cm^2. Macrofossils within the spherule bed represent a rich fauna of ammonites, benthic molluscs (bivalves and gastropods), echinoids, as well as crabs and sharks. Macrofossil preservation ranges from whole to fragmentary, with most fossils preserved as internal moulds. The infill of the fossils is lithologically identical to the matrix of the spherule bed, including impact ejecta preserved within phragmocones and body chambers of ammonites, and differs from the underlying Owl Creek Formation. This suggests that the animals were either alive or loosely scattered on the sea floor at the time of deposition. Grain size changes indicate multiple events were responsible for deposition, and together with taphonomic evidence are consistent with dynamic high energy post-impact processes. Later sea level change during the Paleocene is responsible for a sharp contact at the top of the spherule bed. Geochemical evidence from the Owl Creek and Clayton

Formations at this locality indicate numerous local paleoenvironmental changes affected the Mississippi Embayment at the time of the K–Pg boundary and mass extinction event.

Key words

Cretaceous; Paleogene; ammonite; Chicxulub; impact spherule; mass extinction

1. Introduction

The Cretaceous–Paleogene (K–Pg) mass extinction of 66 Ma is the latest of the 'Big Five' Phanerozoic mass extinction events and was responsible for the loss of ~40% of genera and 76% of species worldwide (Raup and Sepkoski, 1982; Bambach, 2006). The extinction event is intimately linked to abundant evidence in the geologic record worldwide for a catastrophic bolide impact (Alvarez et al., 1980), and the creation of the ~200 km-wide Chicxulub crater on the Yucatan Peninsula, Gulf of Mexico (Fig. 1A) (e.g. Hildebrand et al., 1991; Schulte et al., 2010; Morgan et al., 2016; Renne et al., 2018).

Alternative hypotheses for the cause of this event include longer-term climate or sea level changes, or the deleterious effects arising from the eruption of the Deccan Traps large igneous province in continental India (Schoene et al., 2015; Renne et al., 2015), the bulk of which occurred in a <1 million-year window bracketing the K–Pg boundary. It has also been suggested that a combination of these various factors and events may have led to the mass extinction of an already weakened Cretaceous biosphere (Renne et al., 2013), and even that a causal link may exist between the Chicxulub impact event and the most voluminous eruptions of the Deccan Traps (Richards et al., 2015; Renne et al., 2015). Examining the validity of these various hypotheses has led to vigorous debate in the geological community (e.g. Archibald et al., 2010; Courtillot and Fluteau, 2010; Keller et al., 2010; Bond and Grasby, 2017), with much emphasis placed on the completeness of stratigraphic successions containing the K–Pg boundary, and links between fossil occurrences and sedimentological or geochemical signals of impact and environmental changes during the terminal Cretaceous.

Part of the debate has centred on interpretation of complex K–Pg boundary deposits around the Gulf of Mexico, proximal and intermediate (<5000 km) distance to the Chicxulub crater (Figure 1A) (Schulte et al., 2010). Here siliciclastic units (typically referred to as 'K–Pg Clastic Units' or the 'Clayton Basal Sands' due to their location at the base of the Clayton Formation in the eastern Gulf Coast USA) are commonly present at the K–Pg boundary in a variety of paleoenvironmental settings. These deposits, ranging in thickness from ~10 cm to >5 m, have been interpreted as resulting from dynamic and catastrophic depositional processes directly linked to the bolide impact (e.g. post-impact tsunamis/seiches, platform collapse, mass wasting and debris flows, large storm events) (Smit et al., 1996; Bohor, 1996; Olsson et al., 1996; Schulte et al., 2010; Hart et al., 2012; Yancey and Liu, 2013; Hart et al., 2013; Vellekoop et al., 2014), which fit within an overall model of increasing thickness and depositional energy of impact-related deposits relative to proximity to the Chicxulub crater (Smit et al., 1999; Schulte et al., 2010). Alternative interpretations suggest non-catastrophic processes such as sea level lowstand are responsible for these clastic units, which simply represent incised valley deposits and/or shallow water tempestites during a latest Cretaceous and early Paleocene sea level fall (Mancini et al., 1989; Savrda, 1993; Adatte et al., 1996; Stinnesbeck et al., 2016). If this second scenario is correct, the K–Pg boundary in the region should be marked only by a hiatus, and the record of the mass extinction and associated depositional processes absent due to erosion and reworking.

Focused study of outcrops in the Gulf Coastal Plain of the USA (Fig. 1B) are therefore important to our understanding of Late Cretaceous and early Paleocene environmental change. However, sites in the eastern Gulf Coastal Plain and Mississippi Embayment have received only sporadic attention in the literature due to both a perceived paucity of outcrop, and because of the marked hiatus traditionally suggested by biostratigraphic data based on microfossils and marine molluscs (e.g. Donovan et al., 1988;

Mancini et al., 1989). Recent work, however indicates that many uppermost Maastrichtian successions in this region are abundantly fossiliferous and more biostratigraphically complete than once thought (Hart et al., 2012; Larina et al., 2016), thus providing an important record of marine ecosystems in the region across the K–Pg boundary and associated mass extinction event. Many of these outcrops may also record depositional processes that can be linked directly to the Chicxulub impact event which occurred some 1500 km to the south (Fig. 1A) (Smit et al., 1996; Hart et al., 2013; Sanford et al., 2016), as well as evidence of other environmental changes during this critical time in Earth history.

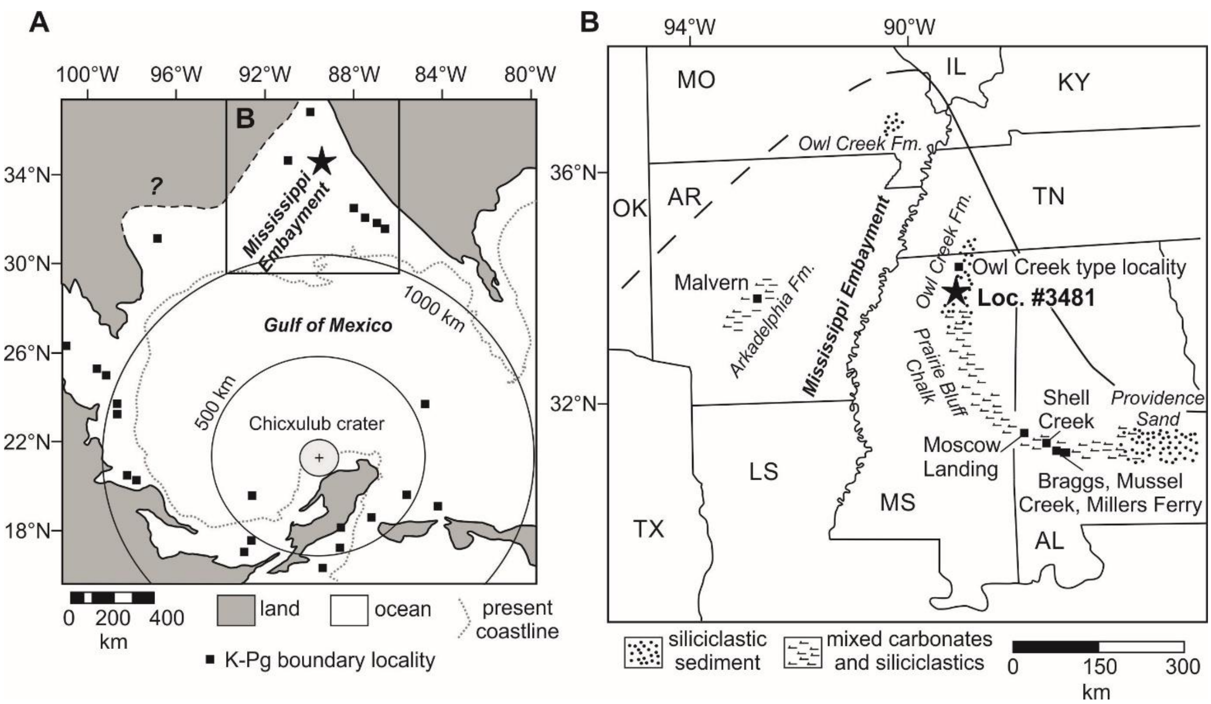

Fig. 1: Geographical and geological setting. (A). Geographic overview of the Gulf of Mexico region, showing both Cretaceous paleogeography in grey and the location of the modern coastline (dashed line). Location of the Chicxulub crater on the Yucatan Peninsula marked by the grey circle with cross, and distances indicated by labelled circles. K–Pg boundary localities from the published literature are indicated by the black squares. AMNH locality 3481 marked with the black star. Inset (B) is indicated. (B). Location map and paleogeography of eastern Gulf Coastal Plain, USA. Inferred position of Cretaceous shoreline marked by solid and dashed black line. K–Pg boundary and other fossiliferous Cretaceous–Paleocene localities mentioned in the text listed. Modified from Larina et al. (2016) and Sandford et al. (2016).

Here we describe a temporary outcrop of the Upper Cretaceous Owl Creek Formation overlain by the lower Paleocene Clayton Formation in Union County, northern Mississippi

(Fig. 1B; Fig. 2). The Owl Creek Formation is abundantly fossiliferous, with both ammonites and a diverse benthic fauna present (e.g. Stephenson, 1955; Sessa et al., 2015). The horizon that forms the contact between these formations is interpreted to mark the K–Pg boundary, and at the locality described herein consists of a poorly sorted quartz sandstone bed 10-30cm-thick, containing abundant impact spherules and marine macrofossils (Fig. 2A, G-H). This unit is similar to other clastic units described from K–Pg boundary successions throughout the Gulf of Mexico and provides an opportunity to study depositional processes behind formation of an event bed containing a rare mixture of well-preserved Chicxulub impact ejecta and a marine fauna.

2. Geological setting

The locality described herein is located in the Mississippi Embayment, a shallow marine basin which stretched from Louisiana into southern Illinois during the Late Cretaceous (Fig. 1). Due to minimal tectonic activity during the last 80 million years, the Embayment preserves an excellent biostratigraphic record of life in the shallow seas which covered the Gulf Coastal Plain region extending back into the Late Cretaceous (Mancini et al., 1995). Maastrichtian (72 – 66 Ma) aged strata in the region are assigned to the Ripley Formation, overlain by the Prairie Bluff Chalk and Owl Creek Formation, and in Arkansas, the age-equivalent Arkadelphia Formation (Pryor, 1960; Puckett 2005; Larina et al., 2016). Stratigraphic relationships between these strata are complex, and in places they are laterally equivalent (Mancini et al., 1996; Larina et al., 2016). All Late Cretaceous deposits are overlain by theClayton and Porters Creek Formations which are Paleocene in age (Mancini et al., 1989; Campbell et al., 2008; Dastas et al., 2014).

The Owl Creek Formation is made up of a sequence of fluvio-deltaic and marginal marine sediments, deposited in the north-eastern part of the Mississippi Embayment with an outcrop area extending from south-eastern Missouri to north-eastern Mississippi (Stephenson and Monroe 1937; Pryor, 1960; Mancini et al., 1996). Biostratigraphic data suggest the formation is late Maastrichtian in age (68 – 66 Ma) (Larina et al., 2016 – see section 5 below), and various lines of evidence indicate a nearshore, shallow marine depositional paleoenvironment (Pryor, 1960; Mancini et al., 1996; Oboh-Ikuenobe et al., 2012; Sessa et al., 2012). On a regional scale (Fig. 1), the upper Maastrichtian of the Mississippi Embayment is generally characterized by a north-south transition from the detrital Owl Creek Formation, to the calcareous Prairie Bluff Chalk and detrital Providence Sand in southern Mississippi and Alabama (Mancini et al., 1996; Larina et al., 2016) (Fig. 1B). An additional distinct facies, known as the 'Nixon Sand', is also present in areas of Mississippi, separating the Prairie Bluff Chalk and Owl Creek Formation (Phillips, 2010). In Mississippi, these upper Cretaceous deposits are disconformably overlain by the siliciclastic Clayton Formation, deposited in a nearshore to neritic paleoenvironment (Mancini et al., 1989; Olsson et al., 1996; Oboh-Ikuenobe et al., 2012). Sequence stratigraphic interpretations of the Gulf Coastal Plain during the Maastrichtian suggest the lower portion of the Owl Creek Formation was deposited during a relative sea level rise representing the transgressive systems tract (TST) (Mancini, 1995). The upper part of the Owl Creek Formation was deposited during the subsequent highstand systems tract (HST) and an overall regressive phase (Mancini et al., 1996; Mancini and Puckett, 2003; Mancini and Puckett 2005; Larina et al., 2016). Deposition of the Clayton Formation above the K–Pg deposits is interpreted to occur during an overall transgressive phase and flooding of the shelf during the early Paleocene (Mancini and Tew, 1993; Schulte and Speijer, 2009).

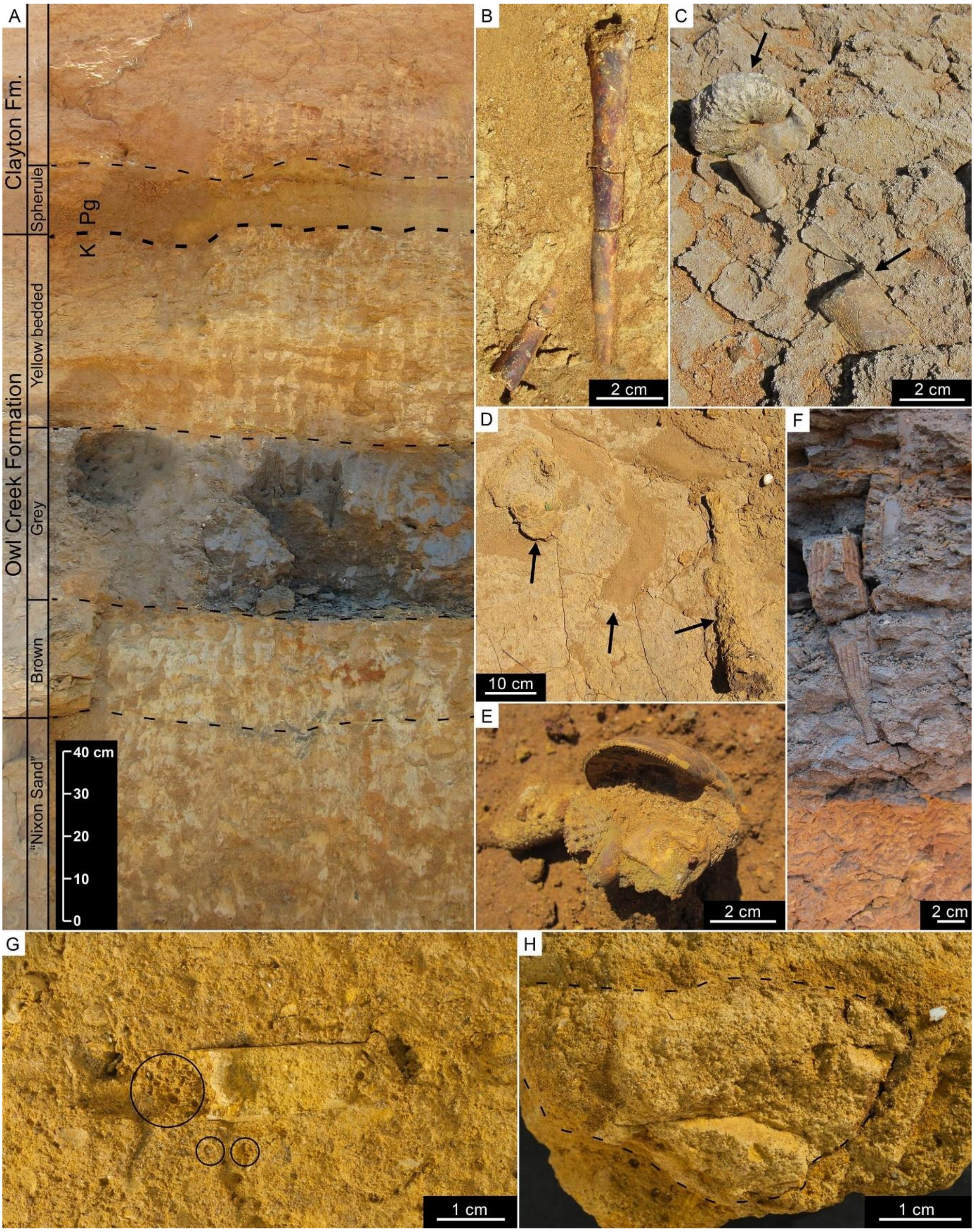

Fig. 2: Outcrop photos of AMNH locality #3481. (A). stratigraphic section through the Owl Creek and basal Clayton Formations showing the distinct lithological units described in the text and the position of the K–Pg boundary (Larina et al., 2016). (B). *Eubaculites* fossil found in the brown unit of the Owl Creek Formation (plan view). (C). Ammonites (*Discoscaphites* and *Eubaculites*) indicated by black arrows, in the grey unit. (D). plan view of a bedding plane in the bioturbated yellow bedded unit with large *Ophiomorpha* burrows marked by arrows. (E). Concentration of fossil molluscs from the spherule bed at the base of the Clayton Formation in-filled with coarse sandstone and impact spherules. (F). Bivalve *Pinna laqueata* in life position at the base of the grey unit. (G). Ammonite

fossil (baculitid) in spherule bed. Spherules marked with black circles. Note presence of spherules and ejecta-bearing lithology infilling the phragmocone. (H). Rip-up clast (outlined with black line) derived from the Owl Creek Formation (including fossil bivalve *Cardium* sp.) within the spherule bed.

The contact between the Owl Creek Formation or Prairie Bluff Chalk and the Clayton Formation in the Gulf Coast is geographically variable (e.g. Stephenson and Monroe, 1940; Stephenson, 1955; Sohl, 1960), and in places there is substantial evidence for a time gap marked by the presence of a lag deposit with phosphatic nodules. Where the basal Clayton Formation is a limestone, it is relatively easy to place the Owl Creek-Clayton formational boundary. Where sand rests upon sand, as at the locality described herein, and there is no evidence for a phosphatic lag deposit, placement of the formational boundary can be challenging. We have chosen to follow Larina et al. (2016) for the placement of this contact (see Section 5 and Discussion below). The surface that forms this boundary has been interpreted by some (e.g. Donovan et al., 1988; Mancini et al., 1989) as a type-1 unconformity and sequence boundary related to eustatic sea level fall at the time of the K–Pg boundary, with overlying clastic units representing incised valley fills deposited during the lowstand systems tract (LST). Alternatively, both these features may be related directly to processes initiated by the Chicxulub impact event (e.g. Smit et al., 1996; Yancey and Liu, 2013; Hart et al., 2012; Hart et al., 2013) and separated from the sequence boundary.

3. Materials and Methods

The exposure is AMNH locality 3481 (referred to as ‘4th Street’ by Larina et al. (2016)) in Union County, between Ripley and the northern edge of New Albany, Mississippi (34°, 29’ 51” north, 88°, 59’ 29” west) (Fig. 1B). Stratigraphic sections were carefully measured in the field using a Jacobs staff and tape measure, recording changes in lithology (Fig. 3), bedding features, and fossil content. A suite of bulk sediment and fossil samples were collected, noting stratigraphic position. Macrofossils were subsequently identified to the lowest taxonomic level possible using the published literature (Stephenson, 1955; Sohl, 1960; Sohl, 1964; Kennedy and Cobban, 2000). For paleoecological analysis of benthic invertebrate macrofossils (bivalves and gastropods), abundance, tiering, feeding mode, and mobility were derived from published sources (e.g. Aberhan and Kiessling, 2015) and supplemented from information contained in the Paleobiology Database (http://fossilworks.org/). These were combined to generate distinct modes of life using the modified categories of Bush et al. (2007) (Table 1). A full faunal list of all invertebrate macrofossils, their abundance, and ecological information is available in Appendix 1. A total of fourteen sediment samples were collected for micropaleontological and biostratigraphic analysis. Key organic-walled dinoflagellate cyst and calcareous nannofossil species from these samples were reported in Larina et al. (2016). Additional details of these samples are noted herein (see Table 2 for details).

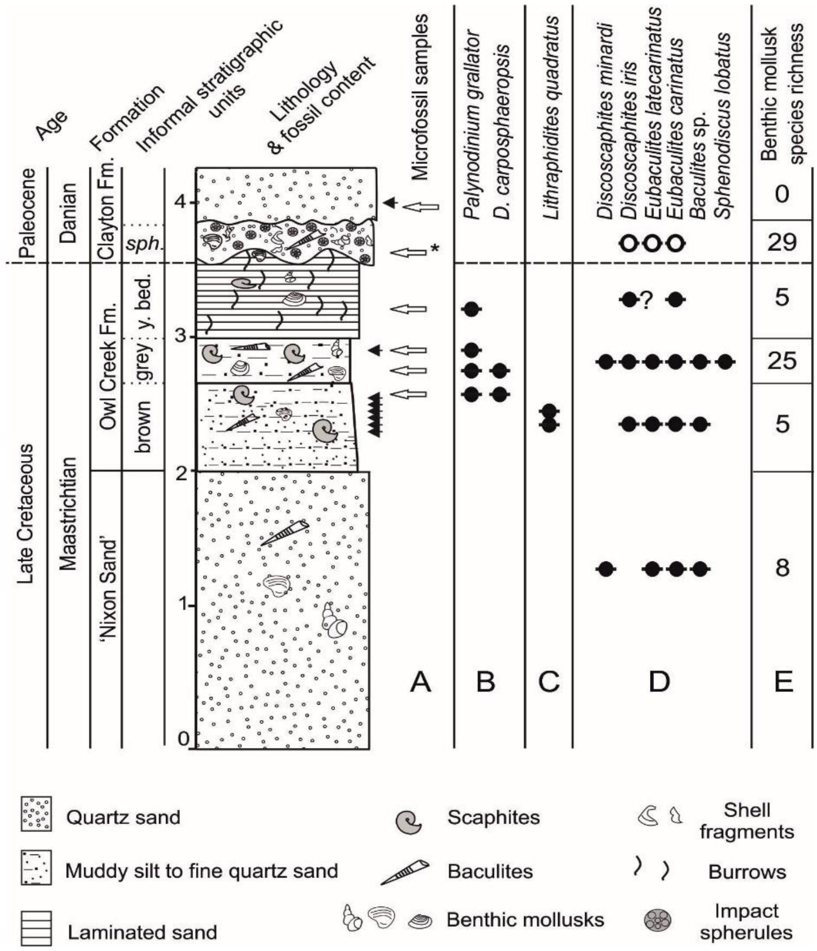

Fig. 3 (previous page): Stratigraphic section of AMNH locality #3481 showing lithologic units, sedimentology, and fossil content. (A). stratigraphic position of samples processed for microfossil analysis. Black arrows = calcareous nannofossils, white arrows = organic-walled dinoflagellate cysts. *indicates that sample comes from the uppermost portion of the yellow bedded unit. (B). stratigraphically important index organic-walled dinoflagellate cysts *D. carposhaeropsis* = *Disphaerogena carposphaeropsis*. (C). stratigraphically important index calcareous nannofossil. See Larina et al. (2016) for a full list of microfossil flora and fauna. (D). index and stratigraphically important ammonite taxa. White circles indicate presence above the K–Pg boundary. (E). species richness of benthic molluscs (bivalves and gastropods).

To elucidate paleoenvironmental and depositional processes, a sub set of sediment samples taken through the Owl Creek and Clayton Formations were sent to the KPESIL lab at the University of Kansas for bulk sedimentary geochemical analysis (organic carbon isotope ($\delta^{13}C_{org}$), total organic carbon (TOC), and carbon/nitrogen ratios (C/N)). Samples were reacted with 0.5 M HCl until all carbonate had reacted, then rinsed with Nanopure water and dried. Samples were weighed, then wrapped in tin capsules and loaded into a Costech Zero Blank Autosampler with continuous flow Ultrapure Helium gas stream. Samples were combusted with an aliquot of oxygen in a Costech Instruments ECS 4010 (Elemental Combustion System). Separated gases were then interfaced via a Thermo Finnigan Conflo III to a Thermo Finnigan MAT 253 Stable Isotope Mass Spectrometer. CO_2 and N_2 gases produced from sample combustion were separated in the GC Column set at 50°C. All samples were analyzed with a suite of both Primary and Secondary (laboratory) stable isotope standards. To determine mineral composition, spherules and fauna from the basal Clayton Formation were examined at the American Museum of Natural History using a Ziess Evo 60 SEM and a Rigaku Micro X-ray Diffractometer.

Concentrations of iridium (Ir) were measured using Inductively Coupled Plasma Mass Spectrometry at the Department of Marine and Coastal Sciences, Rutgers University. Pre-concentration and isolation of Ir from the sediment samples was carried out using a NiS fire-assay technique modified after Ravizza and Pyle (1997). Sediment samples were dried at 105°C overnight, and ~1 g subsample was finely ground and homogenized using an acidcleaned agate mortar and pestle. The resulting powder was then mixed with pure Ni powder and sublimed sulfur (2:1 mass ratio), borax (2:1 ratio to sediment mass), and a ^{191}Ir enriched isotope spike prepared in 6.2N HCl and calibrated against an independent NIST-traceable certified ICP-MS primary Ir standard solution (High-Purity Standards). This mixture was then heated to 1000°C in a muffle furnace for 75 minutes to allow fusion. After fusion and rapid cooling, the glassy sample was broken to release a bead of NiS containing scavenged Ir. Beads were then dissolved in 6.2N HCl at 190 – 200°C on a hot plate until H_2S evolution stops, then were filtered through cellulose 0.45 μm filters (Millipore HATF) to remove small insoluble particles containing much of the Ir. Filters were then digested in concentrated HNO_3 in 15 mL screw-cap Teflon vial (Savillex). Quantification of Ir concentrations used the method of isotope dilution, which provides accurate concentrations even if Ir recovery is low or variable. Multiple full procedural blanks were determined by the same method and the mean subtracted from sample values. Reproducibility of sample analyses was better than ±7%, based on independent analyses of split samples of homogenized powder.

Grain size analysis of the spherule bed was conducted at Brooklyn College. Approximately 50 grams of sediment were taken from seven bulk samples through the uppermost 5 cm of the Owl Creek Formation and basal 30 cm of the Clayton Formation at 5cm stratigraphic intervals. These were physically disaggregated and mixed with a 6% Hexametaphosphate solution for 10 minutes. They were then wet sieved in a 63μm sieve to separate out sand and mud (<63μm) size fractions, and percentages of these grain size fractions were then calculated based on weight loss.

An attempt was also made to estimate the number of impact spherules per cm^2 through the basal Clayton Formation. We prepared an epoxy peel from the surface of an isolated block of the uppermost Owl Creek Formation and basal Clayton Formation. The peel is around 25 cm long, and 2 cm in diameter. The number of spherules up-section were counted from the surface of the peel as an approximation of the density using a 1x1 cm grid, with the results presented as the number of spherules per cm^2. A full list of grain size and spherule surface count data is available in Appendix 3.

4. Results

4.1 Lithological description

4.1.1 'Nixon Sand' and Owl Creek Formation

The measured section at AMNH loc. 3481 is a total of 4.25 m thick (Fig. 2A; Fig. 3), but laterally extensive over several hundred meters. At the base is a 2 m-thick outcrop of the 'Nixon Sand' (Phillips, 2010); an orange-weathering intensely bioturbated calcareous sandstone. Overlying this is a 1.55 m-thick outcrop of the Owl Creek Formation, which at this locality can be divided into three informal units (Fig. 2B-F; Fig. 3). The lowest is a 52.5 cm-thick brown coloured unit, a muddy sandstone that fines upwards to siltstone. Overlying this above a sharp contact is a 35 cm-thick grey unit (Fig 2C; Fig. 3); a micaceous muddy siltstone to very fine quartz sandstone. The grey unit is heavily bioturbated throughout. Large in-situ examples of the semi-infaunal suspension feeding bivalve *Pinna laqueata* are present in the basal 10 cm (Fig. 2F), oriented vertically and apparently in life position.

Above a further sharp contact, the grey unit is overlain by a 67.5 cm-thick yellow bedded unit, which is a laminated but heavily bioturbated sandstone with a mottled appearance in the field. The laminations appear to be thin couplets of coarse and finer-grained material interbedded on a scale of 2–5 cm, and in some places poorly developed cross-beds are apparent. Large *Ophiomorpha* burrow networks occur throughout this unit with a distinctive mamillated exterior surface (Fig. 2D). The sediment infill of these large burrows is the same as the yellow bedded unit. *Ophiomorpha* networks do not descend into the grey unit, abruptly turning before penetrating it. Laminations are less clear in the upper 10 cm of the yellow bedded unit, perhaps due to an increase in the density of small burrows, or because the burrows in this upper interval are more apparent at outcrop and in isolated samples, as they are in-filled with lithologically distinct material from the overlying basal Clayton Formation. This portion of the unit also appears to contain more fossils than the rest of the unit, with several examples of both epifaunal and infaunal bivalves apparently in life position (*Lima acutilineata*, *Anatimya anteradiata*), as well as poorly preserved pectinids and ammonites.

4.1.2 Clayton Formation and spherule bed

The contact at the base of the Clayton Formation is sharp but exhibits undulations on a scale of 5–10 cm (Fig. 2A). Overlying this, the basal Clayton Formation comprises a 10–25 cm-thick poorly sorted, muddy quartz sand with lithic fragments, mica and feldspars (Fig, 4A). This is considered equivalent to the ‘Clayton Basal Sands’ (hereafter referred to as CBS) reported in other publications from numerous localities across the Gulf Coastal Plain (e.g. Mancini et al., 1989; Savrda, 1993; Olsson et al., 1996; Schulte et al., 2006; King and Petruny, 2008; Hart et al., 2013; Larina et al., 2016). This unit contains abundant spherules ranging in size from 0.5 – 1 mm in diameter (Fig. 2G; Fig. 4). Based on their size and distinctive variety of morphologies (Smit et al., 1992; Pitakpaivan et al., 1994; Bohor and Glass, 1995) (see section 4.3 below), these are interpreted to be pseudomorphs of ejecta from the Chicxulub impact event.

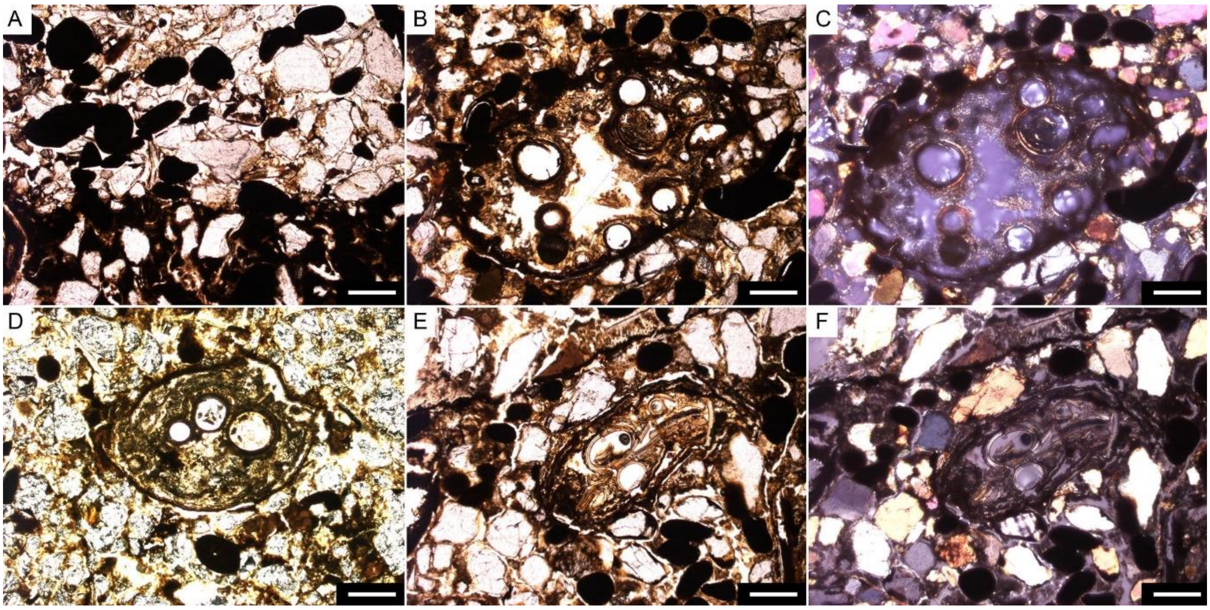

Fig. 4: Thin section photomicrographs of spherule bed microfacies in the basal Clayton Formation. (A). Contact between the yellow bedded unit of the Owl Creek Formation (lower third of the photo) and the spherule bed (Clayton Formation), marked by distinct lithological change in lower portion of the photograph. Dark spheres are glauconitic pellets which occur both below and above the boundary. (B). partially hollow ovoid spherule with some infilling cement, hollow vesicle spherule inclusions and layered rim. Plane polarized light. (C). same image as B but in cross-polarized light. Note compositional banding in walls of vesicular spherules. (D). infilled spherule with hollow vesicular interior structures and distinctive isotropic rim. Set in fine-grained well sorted matrix of quartz, with associated micas and glauconitic pellets (dark spheres), image taken in plane polarized light. (E). Small ovoid spherule showing evidence for plastic deformation and compositional banding. (F). Same image as E in cross polarized light, again showing distinctive banding within vesicular spherule in-fill. All scale bars are 300 µm.

Field examinations and subsequent study of a large isolated block of the uppermost Owl Creek Formation and basal Clayton Formation from AMNH loc. 3481 (Figure 5A) reveal that the spherule bed appears to contain a micro-stratigraphy with at least two distinct subunits’ present in areas where the spherule bed is most expanded (>15 cm thick). These units are defined by changes in colour, sedimentary structures, abundance of impact debris and fossil contact (Figure 5B). A basal 6-7 cm-thick dark orange-red and quartz-rich sand (hereafter referred to as subunit 1) immediately overlies the contact with the Owl Creek Formation, and in-fills large burrows in the upper 10 cm of the underlying yellow bedded unit. The red colour appears to be the result of a (presumably iron-rich) cement. Subunit 1 contains rare impact spherules and fossils. Glauconitic pellets are also common in thin section, with rare micas and feldspars. The dominant constituent is quartz. Above subunit 1, a transition occurs to a 15-17 cm-thick green-pale yellow to dark orange coloured sandstone containing abundant fossils, shell debris and hash, and well-preserved impact spherules, referred to as subunit 2. The contact between the two subunits is mottled and marked by a colour change on fresh surfaces (Fig. 5). This mottling appears to resemble small sedimentary structures - specifically load and flame structures. It could alternatively represent bioturbation, but lack of any evidence for burrowing in the rest of the unit suggests this is unlikely to be the case.

Fig. 5: Stratigraphy, lithology and fossil content of the spherule bed at the base of the Clayton Formation. (A). photograph of isolated block of the uppermost Owl Creek and lower Clayton Formations collected from locality 3481. Annotations related to unit boundaries described in (B). (B). interpretive lithologic column showing fossil content and lithologic changes. See Figure 3 for legend and explanation of symbols. (C). stratigraphic sub-units described in main text. (D). Lithostratigraphy of the spherule bed.

Lithologically the two subunits within the spherule bed are very similar, with subunit 2 again dominantly quartz with glauconite pellets, rare micas and feldspars. Occasional large lithic clasts and altered shell fragments are also present (Fig. 2G; H). Shell fragments and fossils in subunit 2 appear to exhibit a preferred orientation and imbrication, indicative of a current or flow direction. Indistinct laminations are also apparent throughout. The upper ~5 cm of the spherule bed shows a further subtle transition to a dark brown-orange colour sandstone (subunit 2b) although the precise lower boundary of this interval is difficult to place. Subunit 2b also contains abundant impact spherules and imbricated shell fragments. In addition, distinctive grey-white ‘pods’ approximately 2 cm in diameter occur in this interval (Fig. 5A). These do not appear to coincide with a grain size change, but rather local ‘bleaching’ of the sandstone which appears to be a reaction halo caused by penetration of modern plant roots unrelated to Cretaceous–Paleocene depositional processes.

Grain size analysis taken at 5 cm intervals suggest that the spherule bed is lithologically distinct from the uppermost portion of the underlying Owl Creek Formation, with an increase in sand-sized material when compared to a single sample from the yellow bedded unit (Fig. 6A). Several subtle grain size changes are apparent within the spherule bed; one of which appears to coincide with the boundary between subunit’s 1 and 2 (Fig. 5). The spherule bed is capped by an undulating contact with ~3–5 cm of relief, associated with a concentration of imbricated shell debris, the matrix of which appears to be identical to subunit 2 (green-pale yellow sandstone) suggesting subsequent reworking of this interval. Above this contact, the overlying Clayton Formation is composed of 30–55 cm (depending on the thickness of the spherule bed) of unfossiliferous dark orange quartz sand that does not contain impact spherules.

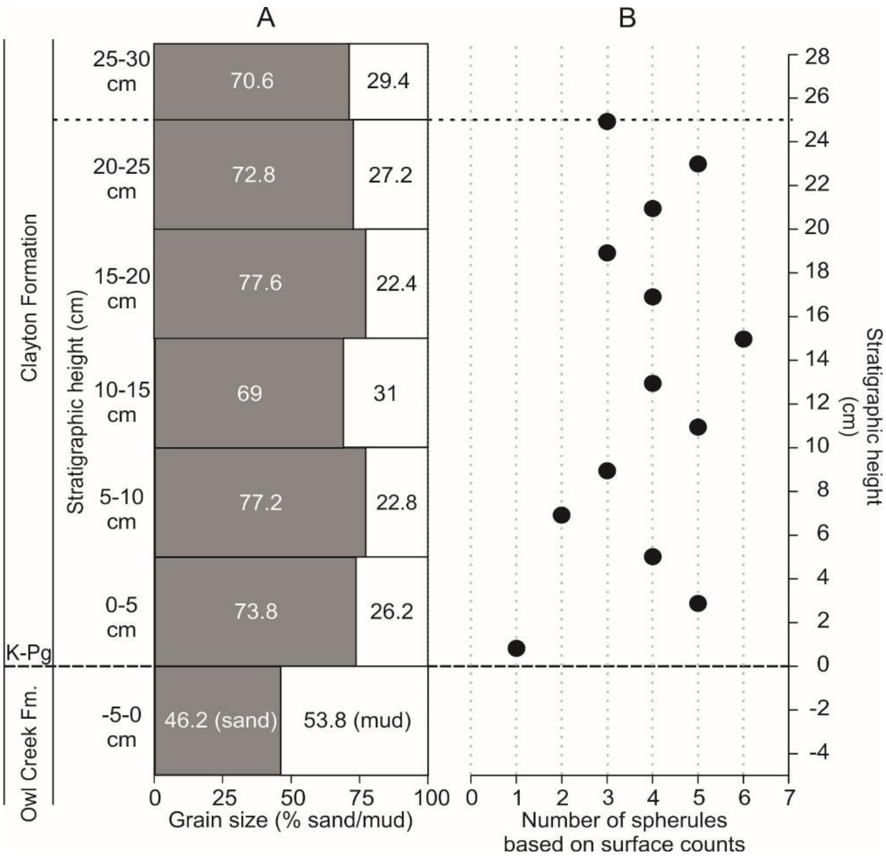

Fig. 6. (A). Grain-size variations (% mud vs. sand-sized material) through the spherule bed of the basal Clayton Formation. (B). surface counts of spherule density, measured from epoxy peel of the surface of the block in Figure 5. No spherules are present in the Owl Creek Formation, or the Clayton Formation overlying the spherule bed.

4.2 Paleontology and paleoecology

The 'Nixon Sand' facies exhibits a moderate fossil content consisting of four species of ammonites, seven species of bivalves, and one gastropod (see Appendix 1 for full list), as well as a dense ichnofauna. Oysters and large irregular echinoids appear to be the most common fossils in the 'Nixon Sand' facies across the region (Phillips, 2010). The basal brown unit of the Owl Creek Formation is also sparsely fossiliferous, but abundance of macrofossils increases up-section to yield a total species richness of six ammonites, four bivalves, and one gastropod (Fig. 3).

The grey unit of the Owl Creek Formation is by contrast, abundantly fossiliferous, with 11 species of cephalopods, including hundreds of examples of the genera *Eubaculites* and *Discoscaphites* (Fig 2C; Fig. 3; Fig.7; Fig. 8). It also contains 19 species of bivalves, six species of gastropods, one species of nautiloid, one species of sponge, crab and vertebrate (marine reptile) remains, as well as fossil wood. All molluscan material is preserved as internal moulds, with no original shell material present. Although the number of ammonites in the collection may represent oversampling, they were the dominant component of this interval. A similar high ratio of ammonites to benthic molluscs has been reported from the Owl Creek type locality in nearby Tippah County (Kennedy and Cobban, 2000; Sessa et al., 2015). Scaphitid ammonites (represented by the genus *Discoscaphites*) are strongly dimorphic (e.g. Landman et al., 2004; Landman et al., 2007), with the dimorphs interpreted as male (microconch) and female (macroconch). The dimorphs are distinguished primarily by the shape of the adult body chamber (see Fig. 7). Of the specimens of *Discoscaphites iris* present in the grey unit, 37% (n = 59) are microconchs, and 63% (n = 102) are macroconchs.

The benthic molluscs in the grey unit exhibit 10 distinct modes of life (Table 1) (Fig. 9). In total 40% of the species are shallow infaunal (10 species), 4% are semi-infaunal (1 species), 44% epifaunal (11 species), and 12% deep infaunal (3 species). Suspension feeding is the most common feeding strategy in this interval at 76% (19 species), compared to 4% which are deposit feeders (1 species) and 20% carnivores (5 species). Overall, the fossil content appears to drop slightly towards the upper portion of the unit. The overlying yellow bedded unit is sparsely fossiliferous but does contain a limited fauna of five species of poorly preserved benthic molluscs and ammonites, including examples of both *Discoscaphites* and *Eubaculites*, three species of bivalves (including several *Exogyra costata* – a bivalve index fossil for the upper Maastrichtian in Mississippi (Stephenson and Monroe, 1940)), and two species of gastropods (Table A4) (Figure 3D).

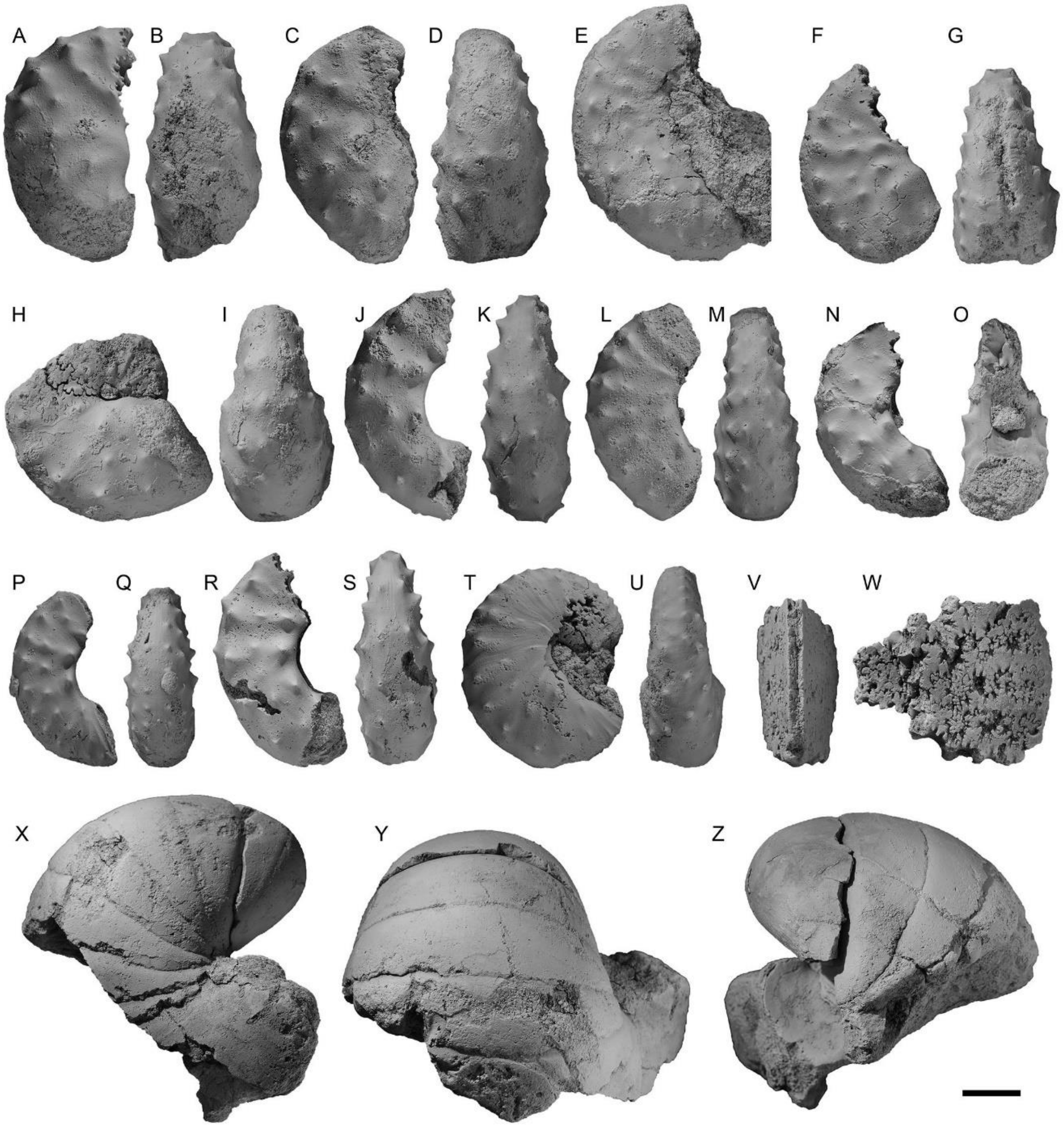

Fig. 7: Ammonites and nautiloid from AMNH loc. 3481. A–U *Discoscaphites iris.* A–I are macroconchs. A–B. AMNH 64572 (grey unit). C–D. AMNH 64543 (grey unit). E. AMNH 64554 (brown unit). F–G. AMNH 64525 (grey unit). H–I. AMNH 64538 (grey unit). J–U are microconchs. J–K. AMNH 64556 (grey unit). L–M. AMNH 64570 (grey unit). N–O AMNH 64553 (brown unit). V–W *Sphenodiscus lobatus.* AMNH 64568 (grey unit). X–Z *Eutrephoceras* sp. AMNH 64567 (grey unit). Scale bar is 1 cm.

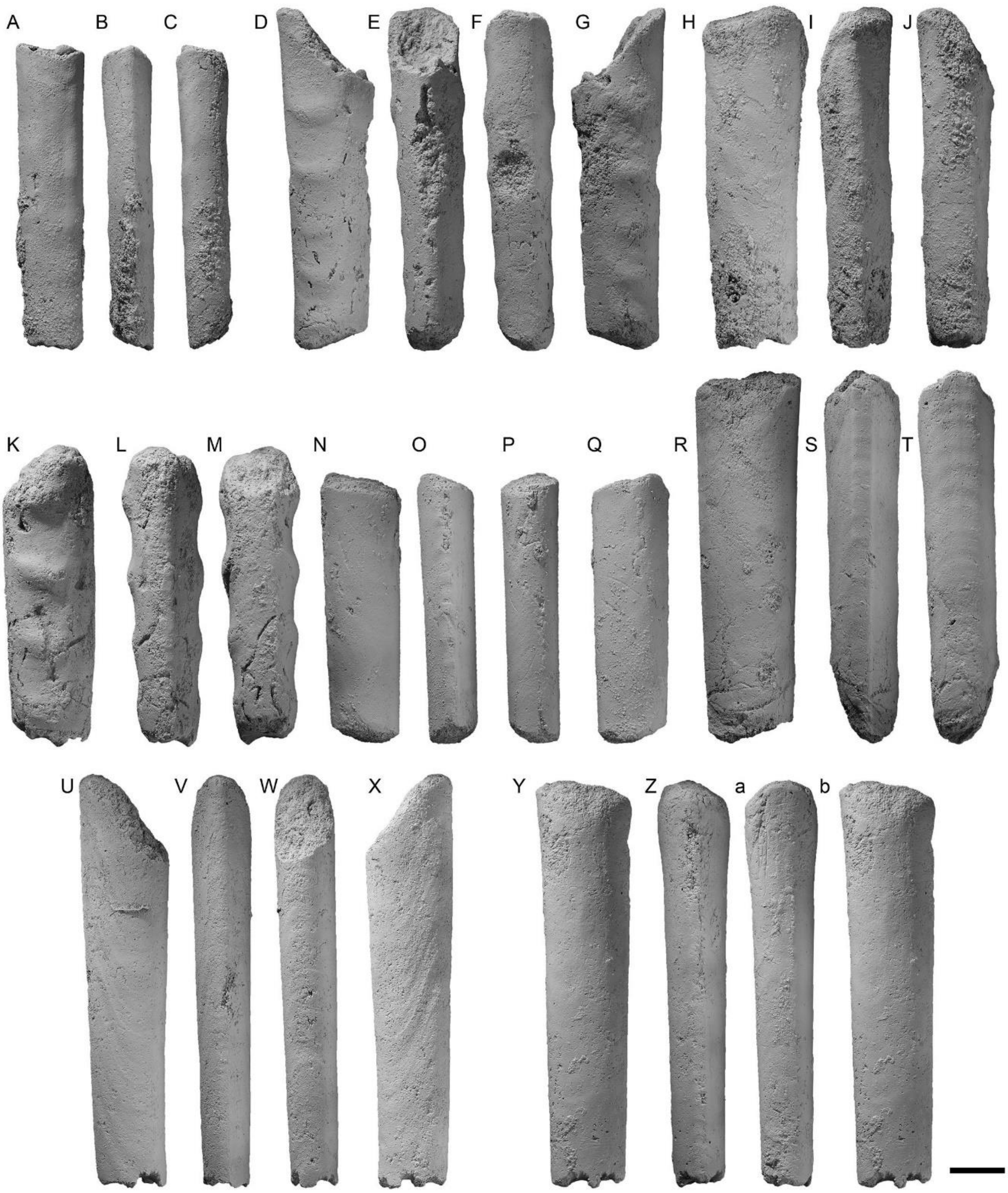

Fig. 8: Ammonites from AMNH loc. 3481. A–M *Eubaculites carinatus*. A–C. AMNH 64411 (grey unit). D–G. AMNH 64481 (grey unit). H–J. AMNH 64599 (grey unit). K–M. AMNH 64453 (grey unit). N–b *Eubaculites latecarinatus*. N–Q. AMNH 64579 (grey unit). R–T. AMNH 64551 (grey unit). U–X. AMNH 64495 (grey unit). Y–b. AMNH 64537 (grey unit). Scale bar is 1 cm.

By contrast, the spherule bed at the base of the Clayton Formation contains an abundant macrofossil fauna consisting of five species of ammonites, 16 species of bivalves, 13 species of gastropods, echinoid fragments and crab remains (Fig. 10). Indeterminate fragments of pectinid bivalves and oysters as well as both scaphitid and baculitid ammonites are also present. This unit is obviously taphonomically complex; it contains shell fragments and debris, but most macrofossils are intact internal molds, some with shell material. Even on partial or broken specimens, delicate structures such as the auricles of pectinid bivalves are commonly preserved. Several larger specimens are in-filled with material clearly derived from the underlying Owl Creek Formation, indicating they represent material reworked as rip-ups (Fig. 2H). The matrix of most of the fossils is however lithologically identical to that of the spherule bed, which appears to argue against significant reworking of the Owl Creek Formation over an extended time interval.

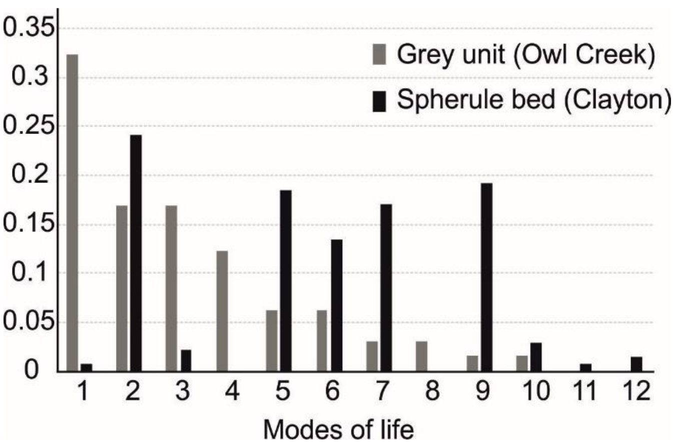

Fig. 9: Proportional abundance of 12 distinct different modes of life exhibited by benthic molluscan taxa (bivalves and gastropods) from the grey unit of the Owl Creek Formation and spherule bed of the basal Clayton Formation. Modes of life are ordered by their abundance in the grey unit from left to right. See Table 1 for key and details of modes of life, which are modified from Bush et al. (2007).

In terms of composition, the fauna is typical of the upper Cretaceous, all species and genera of fossil in the spherule bed are also found in the underlying Owl Creek Formation and units of a similar late Maastrichtian age throughout the Gulf Coastal Plain (e.g. Stephenson, 1955), and no definitively Danian taxa are present. However, the fauna preserved in the spherule bed appears to be subtly different to the most fossiliferous portion of the Owl Creek at this locality (the grey unit) (Appendix 1). A total of 43% of the benthic mollusc species are shallow infaunal (12 species), 54% are epifaunal (15 species) and 4% are semi-infaunal (3 species). Suspension feeders are dominant with 57% (16 species) of the benthos belonging to this feeding mode, compared to 11% that are deposit feeders (3 species), 4% that are herbivores (1 species) and 29% that are carnivores (8 species). The benthic molluscs within the spherule bed belong to 10 distinct modes of life, several of which are not found in the grey unit of the Owl Creek Formation. In addition, the proportional abundance of the different modes of life differs strongly between the two units (Fig. 9), suggesting they represent either two separate communities, or that the fauna in the basal spherule bed represents a community drawn from a larger area than that preserved in the grey unit.

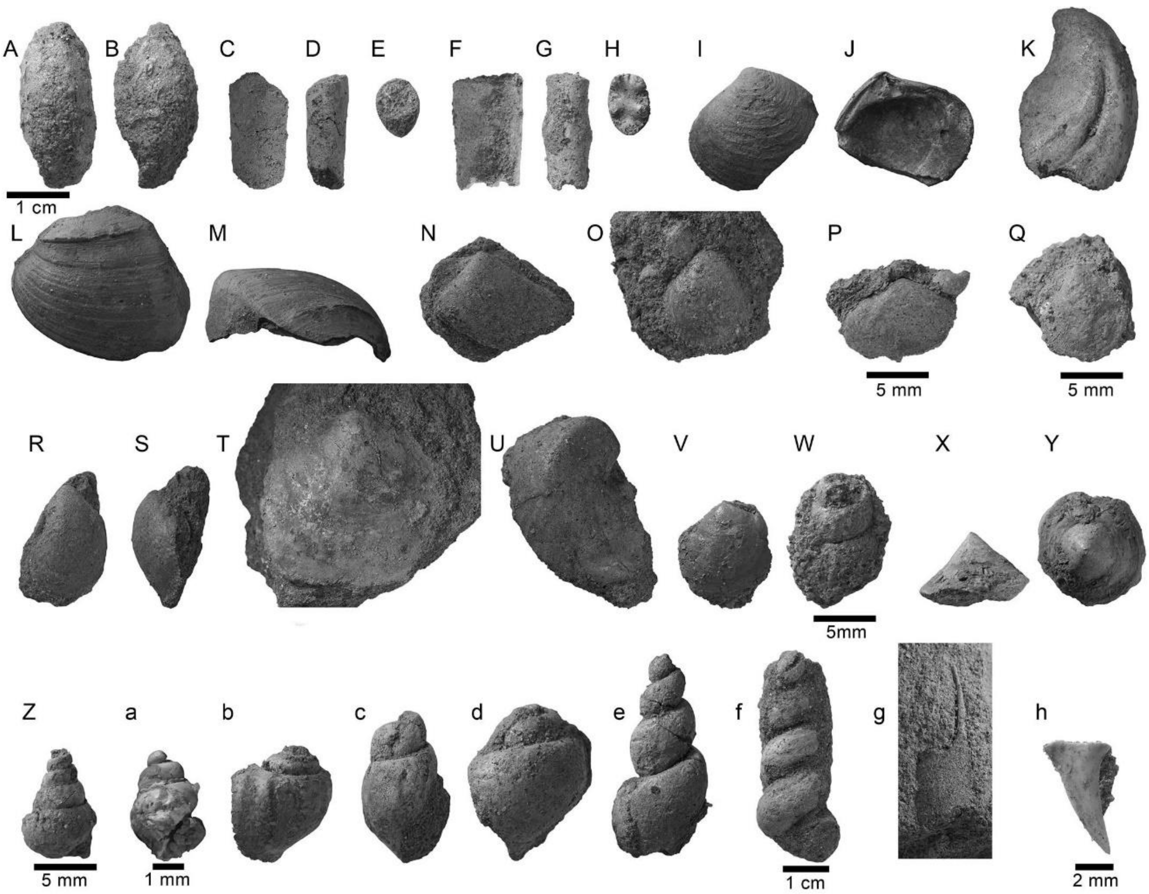

Fig 10: Fossil fauna found in the spherule bed of the basal Clayton Formation at AMNH loc. 3481. A–B. *Discoscaphites iris,* AMNH 85041. C–E. *Eubaculites latecarinatus,* AMMH 85042. F–H. *Eubaculites carinatus*, AMNH 85044A. I–J. *Aphrodina tippana*, AMNH 85039. K. *Cucullaea* sp. AMNH 85038. L–M. *Veniella conradi,* AMNH 85031. N. *Syncyclonema simplicius*? AMNH 85028. O. *Cardium eufalensis,* AMNH 85037. P. *Tellina* sp. AMNH 85036. Q. *Camptonectes bubonis,* AMNH 85030. R–S. *Lima acutilineata,* AMNH 85025. T. *Cypermaria depressa*, AMNH 85027. U. *Exogyra costata*, AMNH 85040. V. *Crassatella* sp. AMNH 85035. W. ?*Anchura* sp. AMNH 85024. X–Y. *Acmaea occidentalis,* AMNH 85023. Z. *Paladmete cancellaria*, AMNH 85022. a. *Anomalofusus*? sp. AMNH 85019. b. *Napulus octoliratus*, AMNH 85015. c. *Arrhoges* (*Latiala*)? sp.

AMNH 85020. d. *Euspira* sp. AMNH 85016. e. *Drilluta major*? AMNH 85021. f. *Turritella vertebroides*, AMNH 85013. g. Indet. Crab. AMNH 85046. h. Indet. Chondrichthyan, AMNH 85045.

4.3 Spherule morphology and composition

Spherules in the basal Clayton Formation at AMNH loc. 3481 are generally very well preserved and show morphologies typical of 'Type 1' Chicxulub impact spherules (c.f. Bohor and Glass, 1995), interpreted as microtektite pseudomorphs of impact melt droplets with distinctive morphologies. These are a characteristic component of many proximal and intermediate K–Pg boundary sites (Bohor and Glass, 1995; Smit et al., 1992; Schulte et al., 2010). The spherules are mostly green-brown or orange in colour, sometimes with a white rim. They range from ~0.5 to 1 mm in diameter. Common morphologies include spheres and spheroids (Fig. 11A), 'dumbells' or examples which appear to be fused spheres (Fig. 11B), ovoids and globular forms (Fig 4B, E). Examination using a binocular microscope, confirmed by thin section and SEM analysis, shows that many spherules are hollow. In other cases, broken or deformed spherules are infilled with siliciclastic material from the matrix of the spherule bed, or with a sparry cement (Fig. 11C-D). Very commonly, large spherules are filled with smaller, vesicular spheres with a similar interior morphology and surface textures leading to an overall 'bubbly' texture. Such features may represent relict gas bubbles (e.g. Smit et al.,1992; Martínez-Ruiz et al., 2001). In thin section the walls of the spherules, and especially the smaller vesicular spherules, appear to show compositional banding when viewed in cross-polarized light (Fig. 4C-F). Despite the remarkably delicate preservation of presumably original features, some spherules show distinct evidence of plastic deformation, presumably caused by sediment loading.

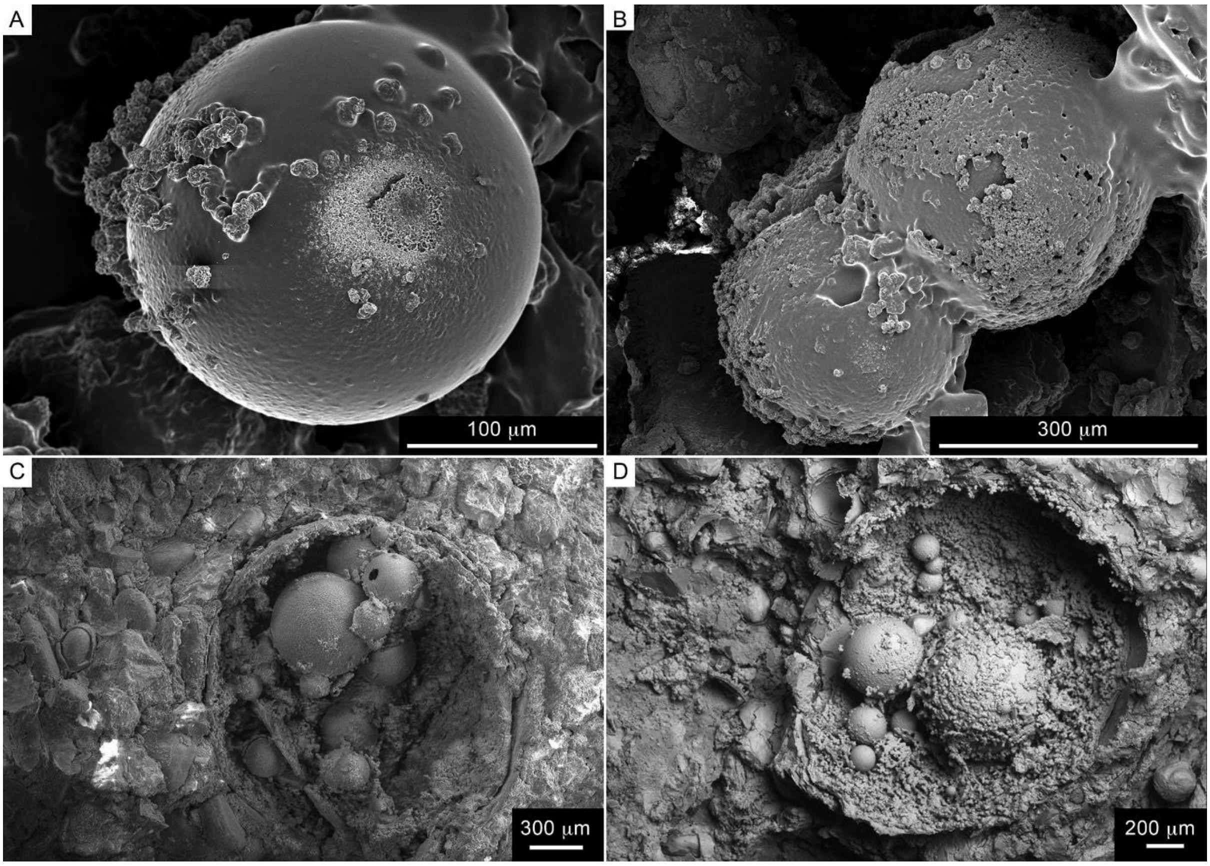

Fig. 11: SEM photographs of impact spherules in the basal Clayton Formation at AMNH locality 3481. (A). typical spherical-shaped spherule extracted from the phragmocone of a baculitid ammonite. Note generally smooth surface with distinctive texture derived from alteration of authigenic smectite. (B). 'Dumbell-shaped' fused spherule with cement overgrowth. (C). Broken spherical-shaped spherule embedded in siliciclastic matrix, showing presence of smaller vesicular spherules in interior. (D). further broken spherule specimen infilled with sparry calcitic cement, again showing smaller vesicular spherules in interior.

XRD analyses confirm the spherules are made up of clay minerals and alteration products such as smectite and montmorillonite, with distinctive 'honeycomb' textures clearly visible in SEM examination (Fig. 11A). Such a composition is in common with the majority of other Chicxulub tektite pseudomorphs at other proximal and intermediate K–Pg boundary sites (e.g. Pitakpaivan et al., 1994; Bohor and Glass, 1995; King and Petruny, 2008) and is a result of alteration from an original glassy precursor material via complex reaction processes during diagenesis (Ferrell et al., 2011; Belza et al., 2015). Within the 10–25 cm-thick spherule bed ejecta is mixed in with the marine fossils, in some cases spherules are even found inside the body chambers and phragmocones of ammonites and the shells of other molluscs, indicating these were hollow at the time of deposition (Fig. 2G).

Spherule density, based on surface counts of a series of epoxy peels through the isolated block shown in Fig. 5, is relatively constant throughout the unit with an average of 4 spherules per cm^2 (Fig. 6B). Density is slightly lower in subunit 1, and in intervals characterized by coarser grain size (Fig. 6A). Spherule diameter also does not appear to change appreciably through the unit, and no grading in terms of spherule size is evident. This is different to deep-sea K–Pg boundary sites which often exhibit a combination of a fining upwards sequences with coincident decreasing spherule diameters (e.g. MacLeod et al., 2007; Schulte et al., 2009) representing settling deposits in a low energy environment.

4.4 Sedimentary geochemistry - $\delta^{13}C_{org}$, TOC, and C/N ratios

Bulk sedimentary $\delta^{13}C_{org}$ values (Fig. 12A) average -24.8 ±1‰ through the Owl Creek and basal Clayton Formations but show distinct variation throughout the section. Values decline by ~1‰ through the brown unit of the Owl Creek Formation to approximately -25.0‰ and show a further sharp drop to -26.4‰ at the base of the grey unit. They generally average -26.0‰ throughout the grey unit, before increasing to -24.7‰ at the base of the yellow bedded unit. From the base to the top of the yellow bedded unit, values show a steady climb by ~+2‰ to a peak of -22.6‰ 15 cm below the contact at the base of the Clayton Formation. A sharp negative excursion of -2‰ occurs in the spherule bed with a minimum value of -26.3‰ at the base. This is followed by two more relatively light values of -24.8 and -24.6‰ 2.5 and 5 cm from the base respectively. In the upper portion of the spherule bed, values return to an average of approximately -23.5‰, and remain the same through the overlying sandstones of the basal Clayton Formation.

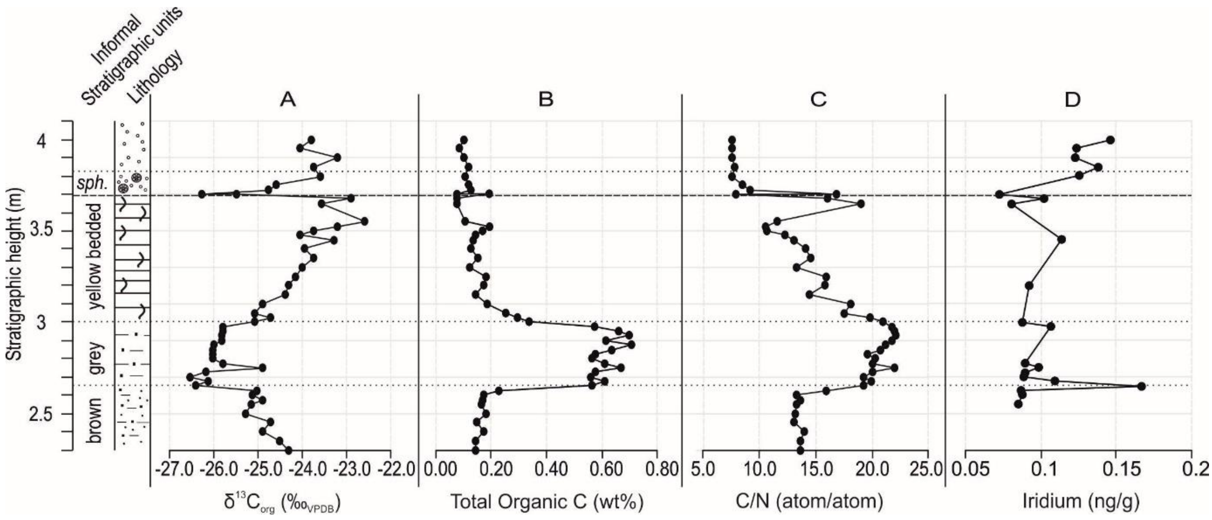

Fig. 12: Sedimentary geochemistry from the Owl Creek and Clayton Formations. Stratigraphic height and informal stratigraphic units refer to sedimentary section outlined on Figure 3. (A). Organic carbon isotopes ($\delta^{13}C_{org}$). (B). Total Organic Carbon (wt%). (C). Carbon:nitrogen ratio (C/N) (atom/atom). (D). Iridium concentration (ng/g). *sph.* = spherule bed.

TOC values (Fig. 12B) are generally low throughout the section, reflecting the sand-rich nature of most of the lithologic units at this site. Values average ~0.15 wt% in the brown and yellow bedded unit but increase to ~0.6 wt% in the grey unit coincident with the negative values expressed by $\delta^{13}C_{org}$. Values of TOC do not show an excursion in the spherule bed coincident with the negative excursion in $\delta^{13}C_{org}$, and this interval exhibits the lowest TOC values that remain relatively consistent through the remainder of the basal Clayton Formation. It should be noted that TOC values could exhibit a diagenetic overprint related to grain size and lithology, with the finer-grained and more clay-rich grey unit preserving a higher proportion of TOC than the sandier brown and yellow bedded units, or the Clayton Formation.

Changes in the C/N ratio of ancient sediments are generally interpreted as reflecting shifting sources of organic matter in ancient marine sediments (e.g. terrestrial vs. marine (Zhan et al., 2011)), with the broad trends considered relatively resistant to diagenetic alteration (e.g. Meyers, 1994). Measurements of C/N ratios (Fig. 12C) in the brown unit of the Owl Creek Formation average 13.7, increasing sharply to 19 in the basal grey unit.

Through the grey unit, values increase further to 22, they then exhibit a gradual decline to a low of 10.5 through the basal 55 cm of the yellow bedded unit. A sharp positive excursion to a value of 16.3, and subsequently 13.7 characterizes the upper 5 cm of the yellow bedded unit. Across the contact at the base of the spherule bed, values fluctuate, ranging from 6.5 to 14.5. They then exhibit an abrupt decline to 7.8 in the upper portion of the spherule bed and remain this low throughout the remainder of the succession.

4.5 Iridium

A total of 21 samples were analyzed for their iridium (Ir) content through the Owl Creek and basal Clayton Formations (Fig. 12D). Most values cluster around an average of 0.105±0.025 ng/g, with a significant peak defined by one data point (0.167 ng/g) occurring at the base of the grey unit. Higher values (closer to 0.15 ng/g) are also present in the spherule bed and the overlying basal Clayton Formation. Even these values are low compared with distal K–Pg boundary sites such as El Kef in Tunisia and Stevns Klint in Denmark (Kiessling and Claeys, 2002; Claeys et al., 2002). The complex stratigraphy of K–Pg clastic units in the Mississippi Embayment likely represent a disturbed environment due to proximity to the Chicxulub crater and high-energy re-deposition. In such settings the primary Ir signal, which is much clearer in distal K–Pg boundary sites (e.g. Smit et al., 1999; Schulte et al., 2010), could be masked by sediment mixing. Erosion due to sea level changes during the Paleocene may also have removed evidence for primary iridium fallout (see section 6.4 below).

5. Biostratigraphy and age model

Multiple lines of evidence from macrofossils (ammonites) and microfossil (organic-walled dinoflagellate cysts (dinocysts) and calcareous nannofossil) fauna and flora suggest that the Owl Creek Formation at this locality was deposited within the final 1 million years or less of the late Maastrichtian. In the study of Larina et al. (2016) the dinoflagellate flora within the Owl Creek Formation was evaluated with reference to the zonation established for the Gulf and Atlantic Coastal Plains (Firth, 1987; Edwards et al., 1999) in the context of the broader compilation assembled by Brinkhuis (2003) (see also FitzPatrick et al., In Press), and additional detail is provided here (see Table 2). The upper part of the brown unit and the grey unit both contain *Palynodinium grallator* (Fig. 3A). A few poorly preserved representatives of this species are also present in the yellow bedded unit. The grey unit also contains examples of *Disphaerogena carposphaeropsis*. The presence of these two species is indicative of the *P. grallator* Zone, which correlates with the upper part of calcareous nannofossil subzones CC26b/UC20d^{TP} and the upper part of the Maastrichtian (see discussion in Edwards et al., 1999; Larina et al., 2016; FitzPatrick et al., In Press). Correlation with magnetostratigraphic records to can provide an additional control on age estimates. In the USGS Santee Reserve Core (Edwards et al., 1999) the first occurrences of *D. carposphaeropsis* and *P. grallator* both occur close to the base of chron C29R, thought to be <500 kyrs prior to the K–Pg boundary (e.g. Schoene et al., 2015).

Calcareous nannofossil biostratigraphy of this site was also discussed by Larina et al. (2016). Rare specimens of *Lithraphidites quadratus* were recovered from the brown unit, 2.35 and 2.45 m above the base of the section (Figure 3B). This species first occurs in nannofossil subzones CC25b and UC20a^{TP} (Perch-Nielsen, 1985; Burnett, 1998). Uppermost Maastrichtian nannofossil markers (e.g. *Micula prinsii*) are absent, but this may be the result of local environmental factors (Larina et al., 2016). Both dinoflagellate cysts and calcareous nannofossils are apparently absent from the Clayton Formation at locality 3481, including the spherule bed. A full list of biostratigraphically important dinoflagellate cyst and calcareous nannofossil taxa from AMNH loc. 3481 and other sites around the Mississippi Embayment can be found in Larina et al. (2016) (see also Table 2).

The age of the macrofossil fauna is consistent with that of the dinocysts and calcareous nannofossils. The presence of abundant representatives of the ammonite

Discoscaphites iris in the brown and grey units of the Owl Creek Formation indicates the *D. iris* Assemblage Zone (Fig. 3C; Fig. 7). This zone is several meters thick in this area although its lower and upper limits are not well documented. This is the highest ammonite zone in North America, representing the uppermost part of the Maastrichtian, and has been shown to consistently correlate with calcareous nannofossil zone CC26b and the *P. grallator* dinocyst zone in both the Atlantic and Gulf Coastal Plains (Landman et al., 2004; Landman et al., 2007; Larina et al., 2016). This combination of key biostratigraphic markers thus suggests that the Owl Creek Formation at AMNH loc. 3481 was likely deposited within just a few hundred kyrs of the K–Pg boundary (see discussion in Larina et al. (2016)).

The associated ammonite fauna in the Owl Creek Formation (Fig. 3C) (*Eubaculites latecarinatus*, *Eubaculites carinatus*, *Sphenodiscus lobatus*, and *Baculites* sp.) is also consistent with uppermost Maastrichtian records from elsewhere in the Gulf and Atlantic Coastal Plains (e.g. Cobban and Kennedy, 1995; Kennedy and Cobban, 2000; Landman et al., 2004a; 2004b; Landman et al., 2007). Ammonites are extremely common in the Owl Creek Formation at AMNH loc. 3481 (Fig. 7; Fig. 8), with hundreds of examples of *Discoscaphites* and *Eubaculites* present in the grey unit. Rare specimens of *Discoscaphites minardi* are found in the 'Nixon Sand' facies and grey unit suggesting that the underlying (older) *D. minardi* Assemblage Zone may be present in this region (Landman et al., 2004a), although it should be noted that *D. minardi* also occurs rarely in the *D. iris* range zone (Landman et al., 2004a; 2004b; Larina et al., 2016).

The appearance of impact ejecta temporally correlates the spherule bed at AMNH loc. 3481 with the Chicxulub impact event, and therefore with the K–Pg GSSP at El Kef in Tunisia (Molina et al., 2006; 2009). It is important to note that Molina et al. (2006) presented two geologically equivalent, but conceptually different definitions for the base of the Danian (p266): "horizon equivalent to the moment of the impact" and "the base of the millimetrethick airfall unit." At El Kef, the moment of impact likely occurred some 40–50 minutes before the deposition of airfall ejecta, based on parameters provided by the Earth Impact Effects Program (https://impact.ese.ic.ac.uk/ImpactEarth/ImpactEffects/) (Collins et al., 2005). These definitions have implications for the precise placement of the boundary in proximal K–Pg sites in the Gulf of Mexico, where ejecta fallout occurred over an even shorter timescale and where these two horizons may be separated by sedimentary sequences deposited in the immediate aftermath of the event (e.g. Smit et al., 1996; Arenillas et al., 2006; Yancey and Liu, 2013).

We follow Larina et al. (2016) in placing the K–Pg boundary at base of the spherule bed (and therefore the Clayton Formation) at AMNH loc. 3481, but recognize there may be alternative placements of the boundary which we discuss below (see sections 6.2 and 6.3). Despite a lack of biostratigraphic control, the sandstones overlying the spherule bed are thought to be equivalent to the Clayton Formation as described elsewhere in the region. Numerous studies have confirmed a Danian age for the lower Clayton Formation in the Mississippi Embayment (e.g. Mancini et al., 1989; Olsson et al., 1996; Schulte and Speijer, 2009; Dastas et al., 2014).

6. Discussion

6.1 Owl Creek Formation and late Maastrichtian paleoenvironments

The Owl Creek Formation at AMNH loc. 3481 is both considerably thinner, and lithologically more variable than at the type locality in nearby Tippah County, where a 9 m-thick succession has been dated to the late Maastrichtian and correlated to calcareous nannofossil zone CC26b, the *Palynodinium grallator* dinocyst zone, and the *D. iris* ammonite range zone (Sessa et al., 2015; Larina et al., 2016). Elsewhere in the northern counties of Mississippi and in adjacent Missouri, the Owl Creek Formation exhibits similar variation in thickness, outcrop extent, fossil content, and lithology (e.g. Stephenson and

Monroe, 1940; Sohl, 1960; Oboh-Ikuenobe et al., 2012). These variations are likely the result of a mixture of factors unique to the local deltaic paleoenvironment, such as shore line topography, variation in sediment supply to the shelf, and differences in accommodation space. Uncertainty still exists concerning the timing and magnitude of climate and sea level changes prior to the K–Pg boundary on a global scale (e.g. Donovan et al., 1988; Olsson et al., 2002; Schulte and Speijer, 2009; Hart et al., 2016; Woelders et al., 2017). Nevertheless, combined fossil and isotopic data in this study provide some support for relatively rapid local changes in paleoenvironment prior to the K–Pg boundary in the Mississippi Embayment.

Overall, the Owl Creek Formation throughout the region represents a shallow and nearshore environment that apparently supported a diverse marine ecosystem during the latest Maastrichtian. Sea-surface temperatures of 26°C and bottom-water temperatures of 19°C are suggested based on molluscan and foraminiferal isotope records from the type locality (Sessa et al., 2015). A shallow paleodepth of <50 m for the succession at AMNH loc. 3481 is consistent with the hypothesised habitat depths of the dominant ammonite taxa (*Discoscaphites* and *Eubaculites*) (Hewitt, 1996; Sessa et al., 2015), as well as many of the benthic molluscs (e.g. *Pinna* (Yonge, 1953)). Fossil abundance is highly variable throughout the 1.5 m-thick succession of the Owl Creek Formation at this locality, with a peak in abundance and species richness in the grey unit (Fig. 3).

Here, a distinct negative shift in $\delta^{13}C_{org}$ and positive TOC values, together with increased C/N ratios (Fig. 12), represent enhanced organic matter preservation as well as changes in sediment supply relative to the underlying brown unit and 'Nixon Sand'. The brown unit exhibits C/N ratios indicative of a mix of marine and terrestrial organic matter, but the elevated values in the grey unit clearly record the increasing influence of terrestrial organic matter, supported by the occurrence of fossil wood in this interval. The greater abundance of suspension feeders over deposit feeders in the rich benthic molluscan fauna indicates a relatively firm substrate, but also suggests that increased input of terrestrial organic matter may have depressed deposit feeding. The occurrence of specimens of *Pinna* apparently in life position at the base of the grey unit (Fig. 2) suggests an autochthonous accumulation, perhaps buried rapidly by increased sediment input from shifting local river systems. The overall drop in fossil content through the unit, together with increasing C/N values, could indicate that repeated pulses of increased sedimentation eventually inhibited all aspects of the community.

Very similar shallow marine communities appear to have developed throughout the Gulf and Atlantic Coastal Plains during the late Maastrichtian (e.g. Landman et al., 2007). These communities are likely to have been influenced not only by periodic fluctuations in local water depth and sedimentation rates, but also changes in terrestrial or riverine input that provided abundant nutrients for the enhanced growth of plankton, which may have been the favoured food of many ammonites (Kruta et al., 2011) as well as other suspension feeders. The paleoecology of ammonites is still debated (e.g. Sessa et al., 2015), but the differing proportions of macro vs microconchs of *Discoscaphites iris* in the grey unit suggests an environmental signal, perhaps sexual segregation of dimorphs related to differing habitat preferences of male and female scaphites.

A conspicuous feature of the geochemical dataset from the Owl Creek Formation is the rapid increase in iridium values at the contact between the brown and grey units to almost double the apparent background level (Fig. 12D). We consider this most likely indicates post-depositional diagenetic remobilization of iridium and concentration at a redox boundary at the contact between the brown and grey units (Colodner et al., 1992), rather than a primary signal of elevated iridium concentrations at this horizon. Similar processes have been suggested for alterations to the impact-induced iridium spike at several distal K–Pg boundary sites (Racki et al., 2010; Miller et al., 2010; Esmeray-Senlet et al., 2017). Iridium may also be associated with detrital clay content in marine sediments (e.g. Alvarez et al., 1990), leading to apparent increases and concentrations in more clay-rich lithologies compared to more sand-rich settings. Field observations, together with the increase in organic matter content, suggest the grey unit is finer-grained and more clay-rich than the sandier brown and yellow bedded units (Fig. 3). Such lithological variation may also be responsible for apparent iridium spikes in the Maastrichtian at other sites on the Gulf Coastal Plain (Donovan et al., 1988).

The general decrease in both macro and microfossil content and preservation, together with a progressive positive shift in $\delta^{13}C_{org}$ and decline in both TOC and C/N ratios through the basal 55 cm of the yellow bedded unit (Fig. 12), could be interpreted as a relatively abrupt change to a more nutrient-poor environment with less terrestrial influence and a greater dominance of marine organic matter compared to the grey unit. This suggests a return to paleoenvironment like that represented by the underlying brown unit, albeit with conditions that favoured poor preservation of both macrofossils and organic-walled dinoflagellate cysts. The presence of weak cross-bedding and repeated changes in grain size indicated by laminations suggest fluctuations in energy levels within the environment of deposition which could account for these features. The yellow bedded unit is also heavily bioturbated (Fig. 2), and the fact that the abundant large *Ophiomorpha* burrows and galleries in this interval do not penetrate the grey unit suggest that it may have been indurated prior to deposition and burrowing. Alternatively, burrowing organisms may have simply not favoured the apparent dominance of terrestrial organic matter preserved in the grey unit.

Such a shift in paleoenvironment most likely represents a change in the source or degree of local terrestrial (riverine) input compared to the grey unit (see Zhan et al. (2011) for a Holocene example). It could also represent a local water depth change, or a mixture of both these scenarios. Numerous estimates of sea level and water depth have been made across the K–Pg boundary along the Gulf and Atlantic Coastal Plains. These suggest that the latest Maastrichtian in the region was characterized by an overall regressive trend (Habib et al., 1996; Olsson et al., 1996; Olsson et al., 2002), with the K–Pg boundary located close to (but not coincident with) a sea level lowstand. At individual sites, the record of water depth changes is more nuanced, and potentially affected by local sequence stratigraphic architecture (e.g. the effect of local delta progradation). For example, in their study of the Antioch Church Core in Lowndes County, Alabama, Schulte and Speijer (2009) note several changes in the latest Maastrichtian which could indicate a deepening of the depositional environment. It is therefore difficult to correlate these short-term changes with global events. An alternative explanation of at least a portion of the yellow bedded unit is that it is related to events surrounding the Chicxulub impact (see section 6.3 below).

6.2 Comparison to other Gulf of Mexico K–Pg boundary sites and impact effects

The spherule bed at AMNH loc. 3481 shows many similarities to other examples of the ‘Clayton Basal Sands’ (CBS) units located stratigraphically above the K–Pg boundary in shallow water settings of the eastern Gulf Coastal Plain (Fig. 1B). Specifically, the lower unit and overlying ‘chaotic’ bed at the Millers Ferry construction site in Wilcox County (Olsson et al., 1996) assigned to early Paleocene biozone P0, the pyrite-rich and overlying spherule-bearing sandstone intervals located directly above the K–Pg boundary in the Antioch Church core (Schulte and Speijer, 2009), the spherule and macrofossil-rich conglomeratic sandstone unit at the base of the Clayton Formation at Moscow Landing (AMNH loc. 3570) (Smit et al.,, 1996; Yancey and Liu, 2013; Hart et al., 2013), and, the spherule and macrofossil-rich unit present at the K–Pg boundary at the Malvern locality in Arkansas (AMNH loc. 3596) (Larina et al., 2016). All resemble the spherule bed at AMNH loc. 3481. The closest comparable succession in terms of depositional setting, thickness and stratigraphy of the K–Pg interval, as well as spherule morphology and density, appears to be the basal spherule-rich bed with entrained macrofossils in the Shell Creek section in Wilcox County, Alabama (King and Petruny, 2008; Ferrell et al., 2011). In deeper water settings, the basal portion (i.e. ‘Unit 1’) of clastic deposits in NE and Central Mexico, which include impact spherules and other ejecta mixed with fossil material derived from shallower water and even terrestrial settings, also seem superficially analogous (e.g. Smit et al., 1992; Smit et al., 1996; Schulte et al., 2012).

However, the bed at AMNH loc. 3481 is clearly different from the complex bioturbated CBS units in the Mussel Creek section in Lowndes County, Alabama (AMNH loc. 3572), which contain early Paleocene (Pα biozone) fossils (Savrda, 1993; Hart et al., 2013). In addition, we do not observe any evidence of thick, graded cross-bedded sand units that often overlie spherule-rich deposits in K–Pg clastic units throughout the Gulf of Mexico (e.g. Smit et al., 1996; Smit, 1999), or the ‘settling layer’ with bioturbation that often caps such K–Pg event beds (Smit et al., 1992; Smit et al., 1996; Arenillas et al., 2006). This highlights one of the difficulties with interpretation of the Clayton Basal Sand units and K–Pg clastic deposits in shallow water settings more generally, in that they can show different lithological characteristics and even evidence for different ages at different sites (Mancini and Tew, 1993; Smit et al., 1996; Schulte and Speijer, 2009; Yancey and Liu, 2013).

The horizon at the base of the spherule bed is laterally extensive over several hundred meters at AMNH loc. 3481 with no evidence of large-scale channelization on the scale of the available outcrop. Burrows immediately below this surface are clearly in-filled with material piped down from the basal portion of the spherule bed (Fig. 5), indicating either a period of erosion, and/or that these burrows were open at the time of deposition. This surface correlates to a regionally extensive feature (Hart et al., 2013), present at the top of the Prairie Bluff Chalk in sedimentary successions in Alabama (Savrda, 1993; Olsson et al., 1996; Schulte and Speijer, 2009; King and Petruny, 2008), and Mississippi (Larina et al., 2016). It also bears similarities to the eroded surface at the top of the Corsicana Formation at the Brazos River sections in Texas (Hart et al., 2012; Yancey and Liu, 2013).

Although this horizon has traditionally been interpreted as a type-1 unconformity related to sea level lowering, with overlying CBS units representing incised valley fills during a sea level lowstand (Donovan et al., 1988; Gale et al., 2006), this hypothesis is not well supported. There is a lack of evidence for sub aerial exposure and channel-like scouring processes attributable to sea level changes at the base of many shallow water K–Pg clastic units in the Gulf Coast, and these deposits often contain marine fossils and indications of bioturbation in at least their upper portions (Savrda, 1993; King and Petruny, 2008). It is therefore considered unlikely that local sea level fell beyond the shelf break at this time (Schulte and Speijer, 2009; Hart et al., 2013). In contrast, this surface could be an erosional feature related directly to the immediate after-effects of the Chicxulub impact (Hart et al., 2016).

The impact event would have produced an immediate magnitude 10-11 earthquake (Day and Maslin, 2005) leading to seismic shaking and ground movement of at least 1-meter vertical displacement up to 7000 km from the crater (Boslough et al., 1996), initiating the collapse of proximal carbonate platforms and mass movement of unconsolidated sediment on and from nearby continental margins as gravity-driven debris flows. The deep Gulf of Mexico acted as a sink for sediment disturbed by seismic shaking and platform collapse, represented today by extensive mass flow deposits (Bralower et al., 1998; Denne et al., 2013; Cobiella-Reguera et al., 2015; Sanford et al., 2016; Poag, 2017). Shallow water sites like those on the Brazos River and at Moscow Landing may also preserve deposits related to seismic disturbance at the base of complex K–Pg boundary event beds (Smit, 1996; Yancey and Liu, 2013), although aspects of complicated local stratigraphy such as faulting remain to be elucidated in some of these successions (Hart et al., 2013).

Both the impact event and subsequent margin collapse had the capacity to trigger the formation of mega-tsunami wave-trains, with the power to scour and redistribute sediments disturbed by earlier seismic shaking, as well as potentially create erosional topography on the shallow sea floor during backflows or related debris flows (Smit et al., 1996; Olsson et al., 1996; Schulte et al., 2012; Hart et al., 2012). The discrete timing of these two processes (seismic disturbance, tsunamis) was probably on the order of minutes to <1 hour following the impact at proximal sites (Collins et al., 2005; Sanford et al., 2016) and, therefore also within the arrival time of coarse ejecta represented by microtektite spherules, which would have begun falling out of the atmosphere at AMNH loc. 3481 (assuming a paleo-distance to Chicxulub of ~1500 km) within 11 minutes (Alvarez et al., 1995; Collins et al., 2005; Artemieva and Morgan, 2009). Seismic disturbance and tsunamis may have persisted for days to weeks after the impact (Renne et al., 2018). Initial deposition and reworking of ejecta-rich deposits would therefore occur on the order of hours to days after the impact – a geological instant.

As noted by Sanford et al. (2016), these three processes (seismic shaking, tsunamis, and air-fall/suspension settling of ejecta and debris) were the primary mechanisms of energy transfer from the impactor to the Earth, and therefore probably the primary initiators of sediment transport and deposition of CBS/K–Pg clastic units around the Gulf of Mexico. In deeper water settings (e.g. Smit et al., 1992; Schulte et al., 2012; Denne et al., 2013; Sanford et al., 2017), a distinct sequence of three to four units can be recognized in clastic units and related to these three processes operating over discrete timescales. In shallow water, it may be difficult to deconvolve the precise nature and timing of different phases of impact-related deposition due to a propensity for repeated high energy reworking. A further complication is evidence for additional reworking by large storm events (Yancey and Liu, 2013), potentially related to climate instability in the immediate aftermath of the impact (e.g. Vellekoop et al., 2014; Brugger et al., 2017).

6.3 Direct evidence for mode of emplacement of spherule bed and depositional processes

Invoking impact-related processes to explain features at AMNH loc. 3481 may also have implications for interpretation of the upper portion of the Owl Creek Formation at this site and the precise placement of the K–Pg boundary. Seismic shaking and disturbance or movement of seafloor sediment, which likely occurred within 5 minutes of the impact event in the Mississippi Embayment (Collins et al., 2005), could be responsible for rapid deposition of at least a portion of the yellow bedded unit. The rapid fluctuations in geochemical variables in the upper portion of the unit, as well as the apparent concentration of macrofossils in this interval provide some support for this. If this scenario is correct, the K–Pg boundary *sensu-stricto* should be placed in the yellow-bedded unit, since as discussed above, the first deposits generated by the impact are defined as the base of the Danian at the K–Pg GSSP at El Kef (e.g. Molina et al., 2006; Arenillas et al., 2006). Evidence for widespread seismic disturbance of Maastrichtian sediments linked to the Chicxulub impact, has recently been recorded by Renne et al. (2018) from K–Pg boundary deposits on Gorgonilla Island in Colombia.

The spherule bed itself shows changes in grain size and lithology which are consistent with the hypothesis that a sequence of multiple, potentially high energy, events were responsible for its formation (Fig. 5; Fig. 6). Separate subunits with subtle grain size changes, and evidence for sedimentary structures indicative of loading could have formed during tsunami backwash events or represent the shallow water expression of hyper-concentrated sand-dominated grain flows which transported and mixed impact ejecta, lithic clasts, and marine animals and macrofossils (Schulte et al., 2012; Yancey and Liu, 2013). Imbrication of fossil material and faint laminations in subunit 2 certainly indicates the presence of a directional current or flow during deposition. Large centimetre-sized clasts of material clearly derived from the underlying Owl Creek Formation (Fig. 2H) are evidence that some higher energy scouring did occur. This also suggests that impact-related processes may have removed or disturbed all unconsolidated and unlithified material prior to deposition of the spherule bed, scouring down into lithified Cretaceous deposits (c.f. Hart et al., 2012).

The composition of the fossil assemblage in the spherule bed, with a broad suite of molluscan macrofossils exhibiting different modes of life (Fig. 9; Fig. 10), is also consistent with transportation and mixing of material from differing water depths and paleoenvironments, as hypothesized for other fossil-bearing K–Pg event beds around the Gulf of Mexico (e.g. Schulte et al., 2012). In general, the spherule bed appears to contain a mix of molluscan taxa from both onshore and offshore settings, which exhibited distinctly differing faunas during the latest Cretaceous (Sessa et al., 2012).

The mixture of macrofossils containing impact ejecta, including impact spherules found within the body chambers and phragmocones of ammonites (Fig 2G), further suggests rapid deposition and infilling of empty shells which were distributed on the sea floor or present in unlithified deposits, as opposed to an extended period of reworking during a sea level fall. This is also supported by the lack of definitive Danian macrofossil markers (e.g. *Ostrea pulaskensis* (Cope et al., 2005)) in the spherule bed. The abundance of ammonites in the Owl Creek Formation, and their presence at the base of the Clayton Formation coincident with impact ejecta at this locality, appears to contradict the argument by Stinnesbeck et al. (2012) that the group suffered a serious decline or pre-extinction at low latitudes prior to the K–Pg boundary. Instead, evidence suggests they remained a part of marine ecosystems in this region right up to the time of the Chicxulub impact.

In the context of the geochemical records (Fig. 12), the K–Pg interval and spherule bed can also be interpreted to represent a rapid perturbation within a longer-term trend of local paleoenvironmental change. $\delta^{13}C_{org}$ values show a sharp negative excursion at the base of the Clayton Formation, combined with fluctuations in TOC and C/N ratios. It is tempting to correlate the negative excursion in $\delta^{13}C_{org}$ to the global negative carbon isotope excursion seen in pelagic carbonates at the K–Pg boundary (e.g. Kump, 1991), but this is not clearly expressed in organic carbon isotope records (Grandpre et al., 2013) due to local processes impacting the bulk sedimentary isotope signal. Changes in these geochemical variables are thus best interpreted as a signature of rapid mixing of organic matter from different sources and paleoenvironments, also consistent with deposition of this interval by impact-related processes outlined above.

6.4 Evidence for early Paleocene sea level change

The sandstones of the Clayton Formation that overlie the spherule bed at AMNH loc. 3481 show $\delta^{13}C_{org}$ values very similar to those recorded in the upper portion of the yellow bedded unit of the Owl Creek Formation, along with low levels of TOC, and C/N ratios indicative of the dominance of marine over terrestrial organic matter (Fig. 12). This is consistent with the overall transgressive interpretation of this interval and a more offshore paleoenvironment. The irregular contact at the top of the spherule bed appears to represent a Danian transgressive surface which may have removed an unknown portion of a once larger clastic unit at this locality – most likely the cross-bedded sand units like those preserved at Shell Creek in Alabama (King and Petruny, 2008; Ferrell et al., 2011) and elsewhere (Smit, 1999), and potentially a ‘settling layer’ which would have contained the undisturbed iridium anomaly (see below).

This transgressive horizon may also correlate with a regional feature which overlies CBS bodies in Alabama and Mississippi and is one of several flooding surfaces that occur within the lower Paleocene deposits of the Gulf Coastal Plain (Smit et al., 1996; Schulte and Speijer, 2009; Leighton et al., 2017), and the Atlantic Coastal Plain (Olsson et al., 2002;

Landman et al., 2007). In places, such as the famous succession at Braggs in Alabama (Jones et al., 1987), this surface appears to merge with the K–Pg boundary, leading to non-deposition (or removal) of the clastic CBS units (Mancini et al., 1989; Olsson et al., 1996; Hart et al., 2013) and complicating their interpretation in a sequence stratigraphic context (Hart et al., 2016). The precise age of this horizon at AMNH loc. 3481 is unknown due to the lack of biostratigraphic control above the K–Pg boundary. Elsewhere the erosion surface has been assigned an age correlating to the P1a foraminiferal zone (Hart et al., 2013; Leighton et al., 2017), several hundred kyrs after the boundary and mass extinction (Arenillas et al., 2004). Identification of this feature is consistent with the findings of Olsson et al. (2002) that the Chicxulub impact and K–Pg boundary do not coincide directly with a sea level fall but are intercalated between sequence boundaries (See also: Schulte et al. (2012); Hart et al. (2014); Hart et al. (2016)).

These conclusions also bear on the interpretation of the upper portion of the iridium profile at AMNH loc. 3481 (Fig. 12). As previously mentioned, in ‘complete’ K–Pg clastic units (e.g. Brazos River, Texas, the El Mimbral and La Lajilla sections, Mexico (Smit et al., 1992; Smit et al., 1996)), the iridium anomaly usually occurs in a ‘carbonate cap’ deposit at the top of the succession, interpreted to represent atmospheric fallout of fine-grained ejecta from suspension. This would have occurred over a period of weeks to months after impact (Smit et al., 1992; Alvarez et al., 1995; Artimieva and Morgan, 2009). The increase in iridium values in the basal part of the Clayton Formation overlying the spherule bed could represent reworking and re-deposition of iridium-rich material associated with the erosion and removal of the upper portion of a once more complete K–Pg clastic unit by the transgressive surface, as opposed to pure fallout from the atmosphere. Again, a lack of age control limits the possible interpretation.

7. Conclusions

We have conducted a detailed analysis of a temporary outcrop of the K–Pg boundary exposed due to construction in Union County, Mississippi, consisting of the Owl Creek Formation and overlying Clayton Formation. The Owl Creek Formation at this locality was deposited in a shallow marine environment, containing a diverse and abundant marine community. The presence of large numbers of the ammonites *Discoscaphites iris* and *Eubaculites carinatus*, along with index dinocysts and calcareous nannofossils, indicate correlation to the upper Maastrichtian *D. iris* Assemblage Zone, the *Palynodinium grallator* dinocyst zone, and deposition within at least the last 1 million years, most likely the last 500 kyrs, of the Cretaceous. Significant facies variability compared to the type section of the Owl Creek Formation in nearby Tippah County, as well as changes in fossil content and variable geochemical data, suggest rapid local paleoenvironmental changes in sediment supply and potentially water depth affected this portion of the Gulf Coastal Plain during the latest Cretaceous, prior to the K–Pg mass extinction.

We interpret the contact at the base of the overlying Clayton Formation as the K–Pg boundary. There is limited evidence for sea level fall beyond the shelf break, or for a significant depositional hiatus (Larina et al., 2016), indicating this surface is unlikely to be a Type-1 unconformity in a sequence stratigraphic context. This surface, and clastic deposits which overlie it, could therefore be the result of dynamic processes related to the Chicxulub impact event – some combination of seismic activity, tsunami waves, and ejecta fallout. The K–Pg boundary is overlain by a sandstone unit containing abundant and well-preserved impact spherules with characteristic morphologies, the first record of Chicxulub ejecta from Mississippi.

An associated rich macrofossil fauna, including benthic molluscs and ammonites in-filled with material containing impact spherules, suggests these animals were alive or loosely scattered on an unlithified sea floor at the time of deposition. The fauna is distinctly different in terms of its composition to that found in the underlying Owl Creek Formation and appears to have been sourced from a wider area or differing paleoenvironmental settings. The admixture of ammonites and Chicxulub impact ejecta strongly suggests these animals remained a significant part of marine ecosystems in this region up to the time of the Chicxulub impact event and K–Pg mass extinction.

Taphonomic, geochemical, and sedimentological evidence from the spherule bed is consistent with deposition by multiple high-energy events in the aftermath of the impact, such as tsunami backwash and/or debris flows initiated as result of tsunami waves or seismic disturbance. Imbrication of fossils, repeated changes in grain size, and the presence of sedimentary structures indicative of loading would suggest rapid deposition, but precise timing is hampered by a lack of biostratigraphic control above the K–Pg boundary. A marine flooding surface which overlies the spherule bed and may have removed a once larger-portion of this clastic unit, is a clear expression of sea level change during the early Paleocene, tens to hundreds of thousands of years after the K–Pg boundary. Future focused study of K–Pg event beds and macrofossil faunas preserved therein has the potential to provide important new information about the timing and nature of depositional processes associated with the Chicxulub impact, and its effects on global marine biota.

Acknowledgements

Thanks to W.C. Smallwood (owner of the site) and George Phillips (Museum of Natural Science, Mississippi) for providing and facilitating access to the field site at AMNH locality 3481, and for help with fossil identification. We thank Corinne Myers, Jone Naujokaityte, the late Susan Klofak, and others for assistance in the field. Morgan Hill and George Harlow (AMNH) are thanked for assistance with SEM imaging and XRD analyses, Steve Thurston (AMNH) for help with figures and photography, and Malinina and Kaixuan

Bu (Rutgers University) for assistance with iridium determinations. We thank the handling editor Dr. Eduardo Koutsoukos and two anonymous reviewers for their helpful comments and suggestions which greatly improved the manuscript. This research was supported by the Lerner-Gray Fund for Marine Research and the Richard Gilder Graduate School, American Museum of Natural History, via a fellowship to James Witts. Additional support was provided by the Norman Newell Fund. Any use of trade, firm, or product names is for descriptive purposes only and does not imply endorsement by the U.S. Government.

References

1. Aberhan, M., and Kiessling, W. 2015. Persistent ecological shifts in marine molluscan assemblages across the end-Cretaceous mass extinction. Proceedings of the National Academy of Sciences 112 (23): 7207–7212.
2. Adatte, T., Stinnesbeck, W., Keller, G. 1996. Lithostratigraphic and mineralogic correlations of near K/T boundary clastic sediments in northeastern Mexico: Implications for origin and nature of deposits. In: Ryder, G., Fastovsky, D., and Gartner, S. (eds.). The Cretaceous-Tertiary Event and other catastrophes in Earth history, Geological Society of America Special Paper 307, Boulder, Colorado: 211–226.
3. Alvarez, L.W., Alvarez, W., Asaro, F., and Michel, H.V. 1980. Extraterrestrial cause for the Cretaceous-Tertiary extinction. Science 208: 1095–1108.
4. Alvarez, W., Claeys, P., Kieffer, S.W. 1995. Emplacement of Cretaceous–Tertiary boundary shocked quartz from Chicxulub crater. Science 269, 930–935.
5. Archibald, J.D., Clemens, W., Padian, K., Rowe, T., Macleod, N., Barrett, P.M., Gale, A., Holroyd, P., Sues, H.-D., and Arens, N.C. 2010. Cretaceous extinctions: multiple causes. Science 328:973.
6. Arenillas, I., Arz, J.A., Molina, E. 2004. A new high-resolution planktic foraminiferal zonation and subzonation for the lower Danian. Lethaia 37, 79–95.
7. Arenillas, I., Arz, J.A., Grajales-Nishimura, J.M., Murillo-Muñetón, G., Alvarez, W., Carmargo-Zanoguera, A., Molina, E., Rosales-Domínguez, C., 2006. Chicxulub impact is Cretaceous/Paleogene boundary in age: new micropaleontological evidence. Earth and Planetary Science Letters 249, 241–257.
8. Artemieva, N., Morgan, J. 2009. Modeling the formation of the K–Pg boundary layer. Icarus 201, 768–780.

9. Bambach, R.K. 2006. Phanerozoic biodiversity mass extinctions. Annual Review of Earth and Planetary Sciences 34: 127–155.

10. Belza, J., Goderis, S., Smit, J., Vanhaecke, F., Baert, K., Terryn, H., and Claeys, P. 2015. High spatial resolution geochemistry and textural characteristics of microtektite: glass spherules in proximal Cretaceous-Paleogene sections: Insights into glass alteration patterns and precursor melt lithologies. Geochimica et Cosmochimica Acta 152: 1–38

11. Bohor, P.F. 1996. A sediment gravity flow hypothesis for siliciclastic units at the K/T boundary, northeastern Mexico. In: Ryder, G., Fastovsky, D., and Gartner, S. (eds.). The Cretaceous-Tertiary Event and other catastrophes in Earth history. Geological Society of America Special Paper 307, Boulder, Colorado: 183–196

12. Bohor, B.F., and Glass, B.P. 1995. Origin and diagenesis of K/T impact spherules: From Haiti to Wyoming and beyond. Meteroritics 30: 182–198.

13. Bond, D.P.G., Grasby, S.E., 2017. On the causes of mass extinctions. Palaeogeography, Palaeoclimatology, Palaeoecology 478, 3–29.

14. Boslough, M.B., Chael, E.P., Trucano, T.G., Crawford, D.A., Campbell, D.L. 1996. Axial focusing of impact energy in the Earth's interior: a possible link to flood basalts and hotspots? *In* Ryder, G., Fastovsky, D., and Gartner, S. (editors), The Cretaceous-Tertiary event and other catastrophes in Earth history. Geological Society of America Special Paper 307: pp. 541–550.

15. Bralower, T.J., Paull, C.K., Leckie, R.M. 1998. The Cretaceous-Tertiary boundary cocktail: Chicxulub impact triggers margin collapse and extensive sediment gravity flows. Geology 26, 331–334.

16. Brinkhuis, H., Sengers, S., Sluijs, A., Warnaar, J., and Williams, G.L 2003. Latest Cretaceous-earliest Oligocene and Quaternary dinoflagellate cysts, ODP Site 1172,

East Tasman Plateau. *In* Exon, N.F., Kennett, J.P., and Malone M.J. (editors), Proceedings of the Ocean Drilling Program, Scientific Results 189 (Online) www.odp.tamu.edu/publications/189_SR/106/106.htm

17. Brugger, J., Feulner, G., Petri, S., 2017. Baby, it's cold outside: Climate model simulations of the effects of the asteroid impact at the end of the Cretaceous. Geophysical Research Letters 44, 419–427.
18. Burnett, J.A., with contributions from Gallagher, L.T., and Hampton, M.J., 1998. Upper Cretaceous. *In* Bown, P.R. (ed.), Calcareous Nannofossil Biostratigraphy, British Micropalaeontological Society Series. Chapman and Hall/Kluwer Academic Publishers, London, pp. 132–199.
19. Bush, A.M., Bambach, R.K., Daley, G.M. 2007. Changes in theoretical ecospace utilization in marine fossil assemblages between the mid-Paleozoic and late Cenozoic. Paleobiology 33, 76–97.
20. Campbell, C.E., Oboh-Ikuenobe, F.E., and Eifert, T.L. 2008. Megatsunami deposit in Cretaceous-Paleogene boundary interval of southeastern Missouri. *In* Evans, K.R., Horton, J.R., Jr., King, D.T., Jr, and Morrow, J.R. (eds.) The sedimentary record of meteorite impacts. The Geological Society of America Special Paper 437, pp 189–198.
21. Claeys, P., Kiessling, W., and Alvarez, W. 2002. Distribution of Chicxulub ejecta at the Cretaceous-Tertiary boundary. *In* Koeberl, C., and MacLeod K.G., eds., Catastrophic Events and Mass Extinctions: Impacts and Beyond: Boulder, Colorado, Geological Society of America Special Paper 356, pp. 55–68.
22. Cobban, W.A., and Kennedy, W.J. 1995. Maastrichtian ammonites chiefly from the Prairie Bluff Chalk in Alabama and Mississippi. Memoir (The Paleontological Society), pp. 1–40.

23. Cobiella-Reguera, J.L., Cruz-Gámez, E.M., Blanco-Bustamante, S., Pérez-Estrada, L., Gil-González, S., Pedraza-Rozón, Y., 2015. Cretaceous-Paleogene boundary deposits and paleogeography in western and central Cuba. Revista Mexicana de Ciencias Geológicas 32, 156–176.

24. Collins, G.S., Melosh, H.J., Marcus, R.A. 2005. Earth Impact Effects Program: A Web-based computer program for calculating the regional environmental consequences of a meteoroid impact on Earth. Meteoritics and Planetary Science 40, 817–840.

25. Cope, K.H., Utgaard, J.E., Masters, J.M., Feldmann, R.M. 2005. The fauna of the Clayton Formation (Paleocene, Danian) of southern Illinois: a case of K/Pg survivorship and Danian recovery. Bulletin of the Mizunami Fossil Museum 32, 97–108.

26. Courtillot, V., and Fluteau, F. 2010. Cretaceous extinctions: The volcanic hypothesis. Science 328 (5981): 973–974.

27. Dastas, N.R., Chamberlain, J.A., and Garb, M.P. 2014. Cretaceous-Paleogene dinoflagellate biostratigraphy and the age of the Clayton Formation, southeastern Missouri, USA. Geosciences 4: 1–29.

28. Day, S., Maslin, M. 2005. Linking large impacts, gas hydrates, and carbon isotope excursions through widespread sediment liquefaction and continental slope failure: The example of the K-T boundary event, *in* Kenkmann, T., Hörz, F., and Deutsch, A., eds., Large meteorite impacts III: Geological Society of America Special Paper 384, p. 239–258.

29. Denne, R.A., Scott, E.D., Eickhoff, D.P., Kaiser, J.S., Hill, R.J., Spaw, J.M. 2013. Massive Cretaceous-Paleogene boundary deposit, deep-water Gulf of Mexico: new evidence for widespread Chicxulub-induced slope failure. Geology 41, 983–986.

30. Donovan, A.D., Baum, G.R., Blechschmidt, G.L., Loutit, T.S., Pflum, C.E., and Vail, P.R. 1988. Sequence stratigraphic setting of the Cretaceous-Tertiary boundary in central Alabama, *in* Wilgus, C.K., Hastings, B.S., Posmaentier, H., Van Wagoner, J., Ross, C.A., and St. Kendall, C.G. (eds.), Sea level changes—An integrated approach. Society of Economic Paleontologists and Mineralogists Special Publication 42, Tulsa, Oklahoma, p. 299–308.

31. Edwards, L.E., Gohn, G.S., Self-Trail, J.M., Prowell, D.C., Bybell, L.M., Bardot, L.P., Firth, J.V., Huber, B.T., Frederiksen, N.O., and MacLeod, K.G., 1999. Physical stratigraphy, paleontology, and magnetostratigraphy of the USGS-Santee Coastal Reserve Core (CHN-803), Charleston County, South Carolina, pp. 1-66. U.S. Geological Survey Open File Report 99–308.

32. Esmeray-Senlet, S., Miller, K.G., Sherrell, R.M., Senlet, T., Vellekoop, J., Brinkhuis, H. 2017. Iridium profiles and delivery across the Cretaceous/Paleogene boundary. Earth and Planetary Science Letters 457, 117–126.

33. Ferrell, R., King, D.T., Petruny, L.W. 2011. Notronitic clay pseudomorphs of Cretaceous–Paleogene (K–T) boundary microtektites, Shell Creek, Alabama, U.S.A. Journal of Sedimentary Research 81, 348–354.

34. Firth, J.V. 1987. Dinoflagellate biostratigraphy of the Maastrichtian to Danian interval in the U.S. Geological Survey Albany Core, Georgia, USA. Palynology 11, 199–216.

35. FitzPatrick, M.E.J., Forber, D.A., Hart, M.B. 2018. Dinocyst stratigraphy and paleoenvironmental interpretation of the Cretaceous/Paleogene boundary at Stevns Klint, Denmark. Cretaceous Research 87, 408-421.

36. Gale, A.S., 2006. The Cretaceous–Paleogene boundary on the Brazos River, Falls County, Texas: is there evidence for impact-induced tsunami sedimentation? Proceedings of the Geologists Association 117, 173–185.

37. Grandpre, R., Schauer, A., Samek, K., Veeger, A., Ward, P., Fastovsky, D. 2013. Testing the terrestrial $\delta^{13}C$ Cretaceous–Paleogene (K–Pg) chemostratigraphic marker. Palaeogeography, Palaeoclimatology, Palaeoecology 381–382, 67–75.

38. Habib, D., Olsson, R.K., Liu, C., Moshkovitz, S. 1996. High-resolution biostratigraphy of sea-level low, biotic extinction, and chaotic sedimentation at the Cretaceous-Tertiary boundary in Alabama, north of the Chicxulub crater. *in* G. Ryder, D. Fastovsky, and S. Gartner, (eds.), The Cretaceous-Tertiary boundary event and other catastrophes in earth history: Geological Society of America Special Paper 307, Boulder, Colorado, p. 243–252

39. Hart, M.B., Yancey, T.E., Leighton, A.D., Miller, B., Liu, C., Smart, C.W., Twitchett R.J. 2012. The Cretaceous-Paleogene boundary on the Brazos River, Texas: New stratigraphic sections and revised interpretations. GCAGS Journal 1, 69-80.

40. Hart, M.B., Harries, P.J., and Cardenas, A.L. 2013. The Cretaceous/Paleogene boundary events in the Gulf Coast: comparisons between Alabama and Texas. GCAGS Transactions 63: 235–255.

41. Hart, M.B., FitzPatrick, M.E.J., and Smart, C.W. 2016. The Cretaceous/Paleogene boundary: foraminifera, sea grasses, sea level change and sequence stratigraphy. Palaeogeography, Palaeoclimatology, Paleoecology 441(3): 420–429.

42. Hewitt, R.A. (1996). Architecture and strength of the ammonite shell. *In* Ammonoid paleobiology: 297–339. Landman, N.H., Tanabe, K. & Davis, R.A. (Eds). New York: Plenum press. pp. 297–339.

43. Hildebrand, A. R., Penfield, G.T., Kring, D.A., Pilkington, M., and Camargo, Z.A. 1991. Chicxulub crater: A possible Cretaceous/Tertiary boundary impact crater in the Yucatan Peninsula. Geology 19: 232–255.

44. Jones, D.S., Mueller, P.A., Bryan, J.R., Dobson, J.P., Channell, J.E.T., Zachos, J.C., Arthur, M.A. 1987. Biotic, geochemical, and paleomagnetic changes across the Cretaceous/Tertiary boundary at Braggs, Alabama. Geology 15: 311–315.

45. Kennedy, W., and Cobban, W.A. 2000. Maastrichtian (Late Cretaceous) ammonites from the Owl Creek Formation in northeastern Mississippi, USA. Acta Geologica Polonica 50: 175–190.

46. Keller G., Adatte, T., Pardo, A., Bajpai, S., Khosla, A., Samant, B. 2010. Cretaceous extinctions: evidence overlooked. Science 328, 974–975.

47. Kiessling, W., and Claeys, P. 2002. A geographic database approach to the KT Boundary. *In* Buffetaut, E., and Koeberl, C. (eds.), Geological and biological effects of impact events, 83–140. Springer, New York.

48. Kring, D. T., and Petruny, L.W. 2008. Impact spherule-bearing Cretaceous–Tertiary sand body, Shell Creek stratigraphic section, Alabama, USA, *in* Evans, K.R., Horton, J.W., King, D.T. Jr., and Morrow, J.R., eds., The Sedimentary Record of Meteorite Impacts: Geological Society of America Special Paper 437, p. 179–187.

49. Kruta, I., Landman, N., Rouget, I., Cecca, F. & Tafforeau, P. (2011). The role of ammonites in the mesozoic marine food web revealed by jaw preservation. Science 331, 70–72.

50. Kump, L.R. 1991. Interpreting carbon-isotope excursions: Strangelove Oceans. Geology 19, 299–302.

51. Landman, N.H., Johnson, R.O., and Edwards, L.E. 2004a. Cephalopods from the Cretaceous/Tertiary boundary interval on the Atlantic Coastal Plain, with a description of the highest ammonite zones in North America. Part 1, Maryland and North Carolina. American Museum Novitates no. 3454.

52. Landman, N.H., Johnson, R.O., and Edwards, L.E. 2004b. Cephalopods from the Cretaceous/Tertiary boundary interval on the Atlantic Coastal Plain, with a description of the highest ammonite zones in North America. Part 2. Northeastern Monmouth County, New Jersey. Bulletin of the American Museum of Natural History 287, 107p.

53. Landman, N.H., Johnson, R.O., Garb, M.P., Edwards, L.E., Kyte, F.T. 2007. Cephalopodsfrom the Cretaceous/Tertiary boundary interval on the Atlantic Coastal Plain, with a description of the highest ammonite zones in North America. Part III. Manasquan River Basin, Monmouth County, New Jersey. Bulletin of the American Museum of Natural History 1–122.

54. Larina, E., Garb, M., Landman, N.H., Dastas, N., Thibault, N., Edwards, L., Phillips, G., Rovelli, R., Myers, C., and Naujokaityte, J. 2016. Upper Maastrichtian ammonite biostratigraphy of the Gulf Coastal Plain (Mississippi Embayment, southern USA). Cretaceous Research 60: 128–151.

55. Leighton, A.D., Hart, M.B., Smart, C.W., Leng, M.J., Hampton, M. 2017. Timing recovery after the Cretacuos/Paleogene boundary: evidence from the Brazos River, Texas. Journal of Foraminiferal Research 47, 229–238.

56. MacLeod, K. G., Whitney, D.L., Huber, B.T., and Koeberl, C. 2007, Impact and extinction in remarkably complete Cretaceous-Tertiary boundary sections from Demerara rise, tropical western North Atlantic: Geological Society of America, Bulletin 119: 101–115.

57. Mancini, E.A., Tew, B.H., and Smith, C.C. 1989. Cretaceous-Tertiary contact, Mississippi and Alabama. The Journal of Foraminiferal Research 19: 93–104.

58. Mancini, E.A. 1995. Geochronology, biostratigraphy and sequence stratigraphy of a marginal marine to marine shelf stratigraphic succession: Upper Paleocene and lower

Eocene, Wilcox Group, eastern Gulf Coastal Plain, U.S.A. Society for Sedimentary Geology Special Publication 54: 281–293.

59. Mancini, E.A., Puckett, T.M., and Tew, B.H. 1996. Integrated biostratigraphic and sequence stratigraphic framework for Upper Cretaceous strata of the eastern Gulf Coastal Plain, USA. Cretaceous Research 17(6):645–669.

60. Mancini, E.A., and Puckett, T.M., 2003. Integrated biostratigraphic and sequence stratigraphic approach for correlation and basin interpretation. Gulf Coast Association of Geological Societies Transactions 53: 517–526.

61. Mancini, E.A., and Puckett, T.M., 2005. Jurassic and Cretaceous transgressive-regressive (TR) cycles, northern Gulf of Mexico, USA. Stratigraphy 2: 31–48.

62. Martinez-Ruiz, F., Ortega-Huertas, M., Kroon, D., Smit, J., Palomo-Delgado, I., Rocchia, R., 2001. Geochemistry of the Cretaceous–Tertiary boundary at Blake Nose (ODP Leg 171B). *In*: Kroon, D., Norris, R.D., Klaus, A. (Eds.), Western North Atlantic Paleogene and Cretaceous Paleoceanography, Special Publication, vol. 183. Geological Society of London, London, United Kingdom, pp. 131–148.

63. Meyers, P.A. 1994. Preservation of elemental and isotopic source identification of sedimentary organic matter. Chemical Geology 114, 289–302.

64. Miller, K.G., Sherrell, R.M., Browning, J.V., Field, M.P., Gallagher, W., Olsson, R.K., Sugarman, P.J., Tuorto, S., and Wahyudi, H. 2010. Relationship between mass extinction and iridium across the Cretaceous–Paleogene boundary in New Jersey. Geology 38: 867–870.

65. Molina, E., Alegret, L., Arenillas, I., Arz, J.A., Gallala, N., Hardenbol, J., Salis, K.v., Steurbaut, E., Vandenberghe, N., and Zaghbib-Turki, D., 2006. The Global Boundary Stratotype Section and Point for the base of the Danian Stage (Paleocene, Paleogene,

"Tertiary", Cenozoic) at El Kef, Tunisia-Original definition and revision. Episodes 29: 263–273.

66. Molina, E., Alegret, L., Arenillas, I., Arz, J.A., Gallala, N., Grajales-Nishimura, J.M., Murillo-Muňetón, Zaghbib-Turki, D. 2009. The Global Boundary Stratotype Section and Point for the base of the Danian Stage (Paleocene, Paleogene, "Tertiary", Cenozoic): auxiliary sections and correlation. Episodes 32: 84–94

67. Morgan, J.V., Gulick, S.P.S., Bralower, T., Chenot, E., Christeson, G., Claeys, P., Cockell, C., Collins, G.S., Coolen, M.J.L., Ferrière, L., Gebhardt, C., Goto, K., Jones, H., Kring, D.A., Le Ber, E., Lofi, J., Long, X., Lowery, C., Mellett, C., Ocampo-Torres, R., Osinski, G.R., Perez-Cruz, L., Pickersgill, A., Poelchau, M., Rae, A., Rasmussen, C., Rebolledo-Vierya, M., Riller, U., Sato, H., Schmitt, D.R., Smit, J., Tikoo, S., Tomioka, N., Urrutia-Fucugauchi, J., Whalen, M., Wittmann, A., Yamaguchi, K.E., Zylberman, W. 2016. The formation of peak rings in large impact craters. Science 354: 878–882.

68. Oboh-Ikuenobe, F.E., Spencer, M.K., Campbell, C.E., and Haselwander, R.D. 2012. A portrait of late Maastrichtian and Paleocene palynoflora and paleoenvironment in the northern Mississippi Embayment, southeastern Missouri. Palynology 36: 63–79.

69. Olsson, R.K., Liu, C., and van Fossen, M. 1996, The Cretaceous-Tertiary catastrophic event at Miller's Ferry, Alabama, *in* G. Ryder, D. Fastovsky, and S. Gartner, (eds.), The Cretaceous-Tertiary boundary event and other catastrophes in earth history: Geological Society of America Special Paper 307, Boulder, Colorado, p. 263–277.

70. Olsson, R.K., Miller, K.G., Browning, J.V., Wright, J.D., Cramer, B.S., 2002. Sequence stratigraphy and sea-level change across the Cretaceous-Tertiary boundary on the New Jersey passive margin. In: Koeberl, C., MacLeod, K.G. (Eds.),

Catastrophic Events and Mass Extinctions: Impacts and Beyond: Geological Society of America Special Paper 356, Boulder Colorado, pp. 97-108.

71. Perch-Nielsen, K. 1985. Mesozoic calcareous nannofossils. *in* Bolli, H.M., Saunders, J.B., and Perch-Nielsen, K. (eds.), Plankton stratigraphy. Cambridge University, Cambridge.
72. Phillips, G.E. 2010. A distinctive lithofacies between the Prairie Bluff and Owl Creek Formations (Upper Cretaceous) of north Mississippi and its characteristic faunal content. Journal of the Mississippi Academy of Sciences. Abstracts with Program 55: 78.
73. Pitakpaivan, K., and Hazel, J.E., 1994. Ostracodes and chronostratigraphic position of the Upper Cretaceous Arkadelphia Formation of Arkansas. Journal of Paleontology 111–122.
74. Poag, C.W. 2017. Shaken and stirred: Seismic evidence of Chicxulub impact effects on the West Florida carbonate platform, Gulf of Mexico. Geology 45, 1011–1014.
75. Pryor, W.A. 1960. Cretaceous sedimentation in upper Mississippi Embayment. Bullletin of the American Association of Petroleum Geologists 44: 1473–1504.
76. Puckett, T.M. 2005. Santonian-Maastrichtian planktonic foraminiferal and ostracode biostratigraphy of the northern Gulf Coastal Plain, USA. Stratigraphy 2: 117–146.
77. Racki, G., Machalski, M., Koeberl, C., and Harasimiuk. M. 2010. The weathering−modified iridium record of a new Cretaceous–Palaeogene site at Lechwka near Chełm, SE Poland, and its palaeobiologic implications. Acta Palaeontologica Polonica 56: 205–215.
78. Raup, D.M., and Sepkoski, J.J. 1982. Mass extinctions in the marine fossil record. Science 215 (4539): 1501–1503.

79. Ravizza, G., Pyle, D. 1997. PGE and Os isotopic analyses of single sample aliquots with NiS fire assay preconcentration. Chemical Geology 141, 251–268.

80. Renne, P.R., Deino, A.L., Hilgen, F.J., Kuiper, K.F., Mark, D.F., Mitchell, W.S. III, Morgan, L.E., Mundil, R., and Smit, J. 2013. Time Scales of Critical Events Around the Cretaceous-Paleogene Boundary. Science 339: 684–687.

81. Renne, P.R., Sprain, C.J., Richards, M.A., Self, S., Vanderkluysen, L., and Pande, K. 2015. State shift in Deccan volcanism at the Cretaceous-Paleogene boundary, possibly induced by impact. Science 350: 76–78.

82. Renne, P.R., Arenillas, I., Arz, J.A., Vajda, V., Gilabert, V., Bermúdez, H.D., 2018. Multiproxy record of the Chicxulub impact at the Cretaceous-Paleogene boundary from Gorgonilla Island, Colombia. Geology 46, 547e550.

83. Richards, M.A., Alvarez, W., Self, S., Karistrom, L., Renne, P.R., Manga, M., Sprain, C.J., Smit, J., Vanderkluysen, L., and Gibson, S.A. 2015. Triggering of the largest Deccan eruptions by the Chicxulub impact. Geological Society of America Bulletin 127: 1507–1520.

84. Sanford, J.C., Snedden, J.W., Gulick, S.P.S., 2016. The Cretaceous-Paleogene boundary deposit in the Gulf of Mexico: large-scale oceanic basin response to the Chicxulub impact. J. Geophys. Res. Solid Earth 121 (3):1240–1261.

85. Savrda, C. E., 1993, Ichnosedimentologic evidence for a noncatastrophic origin of Cretaceous-Tertiary boundary sands in Alabama. Geology 21: 1075–1078.

86. Schoene, B., Samperton, K.M., Eddy, M.P., Keller, G., Adatte, T., Bowring, S.A.,Khadri, S.F., and Gertsch, B., 2015. U-Pb geochronology of the Deccan Traps and relation to the end-Cretaceous mass extinction. Science 347: 182–184.

87. Schulte P., Speijer R.P. 2009. Late Maastrichtian-Early Paleocene sea level and climate changes in the Antioch Church Core (Alabama, Gulf of Mexico margin, USA): a multi-proxy approach. Geologica Acta 7, 11−34.

88. Schulte, P., Deutsch, A., Salge, T., Berndt, J., Kontny, A., MacLeod, K.G., Neuser, R.D., Krumm, S. 2009. A dual-layer Chicxulub ejecta sequence with shocked carbonates from the Cretaceous−Paleogene (K−Pg) boundary, Demerara Rise, western Atlantic. Geochimica Cosmochimica Acta 73, 1180−1204.

89. Schulte, P., Alegret, L., Arenillas, I., Arz, J.A., Barton, P.J., Bown, P.R., Bralower, T.J., Christeson, G.L., Claeys, P., Cockell, C.S., Collins, G.S., Deutsch, A., Goldin, T.J., Goto, K., Grajales−Nishimura, J.M., Grieve, R.A.F., Gulick, S.P.S., Johnson, K.R., Kiessling, W., Koeberl, K., Kring, D.A., MacLeod, K.G., Matsui, T., Melosh, J., Montanari, A., Morgan, J.V., Neal, C.R., Nichols, D.J., Norris, R.D., Pierazzo, E., Ravizza, G., Rebolledo−Vieyra,M., Reimold, W.U., Robin, E., Salge, T., Speijer, R.P., Sweet, A.R., Urrutia−Fucugauchi, J., Vajda, V., Whalen, M.T., and Willumsen, P.S. 2010. The Chicxulub asteroid impact and mass extinction at the Cretaceous–Paleogene Boundary. Science 327: 1214–1218.

90. Schulte, P., Smit, J., Deutsch, A., Salges, T., Friese, A., Beichel, K. 2012. Tsunami backwash deposits with Chicxulub impact ejecta and dinosaur remains from the Cretaceous–Palaeogene boundary in the La Popa Basin, Mexico. Sedimentology 59: 737–765.

91. Sessa, J.A., Bralower, T.J., Patzkowsky, M.E., Handley J.C., and Ivany, L.C., 2012. Environmental and biological controls on the diversification and ecological reorganization of Late Cretaceous and early Paleogene marine ecosystems in the Gulf Coastal Plain. Paleobiology 38: 218–239.

92. Sessa, J.A., Larina, E., Knoll, K., Garb, M.P., Cochran, K., Huber, B.T., MacLeod, K.G., and Landman, N.H., 2015. Ammonite habitat revealed via isotopic composition and comparisons with co-occurring benthic and planktonic organisms. Proceedings of the National Academy of Sciences of the United States of America 112: 15562–15567.

93. Sohl, N.F. 1960. Archeogastropoda, Mesogastropoda, and stratigraphy of the Ripley, Owl Creek and Prairie Bluff formations. U.S. Geological Professional Paper 331-A: 1–151.

94. Sohl, N.F., 1964, Neogastropoda, Opisthobranchia and Basommatrophora from the Ripley, Owl Creek, and Prairie Bluff Formations, Late Cretaceous gastropods in Tennessee and Mississippi. U.S. Geological Survey Professional Paper 331-B, p. 153–330.

95. Smit, J., Montanari, A., Swinburne, N.H.M., Alvarez, W., Hildebrand, A.R., Margolis, S.V., Claeys, P., Lowrie, W., and Asaro, F. 1992. Tektite-bearing, deep-water clastic unit at the Cretaceous-Tertiary boundary in northeastern Mexico. Geology 20: 99–103.

96. Smit, J., Roep, T.B., Alvarez, W., Montanari, A., Claeys, P., Grajales-Nishmura, J.M., and Bermudez, J. 1996. Coarse grained clastic sandstone complex at the K/T boundary around the Gulf of Mexico: Deposition by tsunami waves induced by the Chicxulub impact? *In* Ryder, G., Fastovsky, D., and Gartner, S. (editors), The Cretaceous-Tertiary event and other catastrophes in Earth history. Geological Society of America Special Paper 307: 151–182.

97. Smit, J. 1999. The global stratigraphy of the Cretaceous-Tertiary boundary impact ejecta. Annual Review of Earth and Planetary Sciences 27: 75–113.

98. Stephenson, L.W., 1955. Owl Creek (Upper Cretaceous) fossils from Crowleys Ridge, southeastern Missouri. U.S. Geological Survey Professional Paper 274: 97–140.

99. Stephenson, L.W., and Monroe, W.H. 1937. Stratigraphy of Upper Cretaceous series in Mississippi. Bulletin of the Association of American Petroleum Geology 22(12): 1639–1657

100. Stephenson, L.W., and Monroe, W.H. 1940. The Upper Cretaceous Deposits. Mississippi Geological Survey, University Mississippi. Bulletin 40: p.293

101. Stinnesbeck, W., Ifrim, C., Salazar, C. 2012. The last Cretaceous ammonites in Latin America. Acta Palaeontologica Polonica 57, 717–728.

102. Stinnesbeck, W., Frey, E., Espinoza-Chávez, Zell, P., Flores-Ventura, J., Rivera-Sylva, H.E., González-González, A.H., Padilla Gutierrez, J.M., Vega, F.J. 2016. Theropod, avian, pterosaur, and arthropod tracks from the uppermost Cretaceous Las Encinas Formation, Coahuila, northeastern Mexico, and their significance for the end-Cretaceous mass extinction. Geological Society of America Bulletin 129, 331–348.

103. Vellekoop, J., Sluijs, A., Smit, J., Schouten, S., Weijer, J.W.H., Sinninghe Damsté, J.S., and Brinkhuis, H. 2014. Rapid short-term cooling following the Chicxulub impact at the Cretaceous–Paleogene boundary. Proceedings of the National Academy of Sciences of the United States of America 111, 7537–7541.

104. Woelders, L., Vellekoop, J., Kroon, D., Smit J., Casadio, S., Prámparo, M. B., Dinares-Turell, J., Peterse, F., Sluijs, A., Lenaers, J.T.M., Speijer, R.P. 2017. Latest Cretaceous climatic and environmental change in the South Atlantic region. Paleoceanography, doi: 10.1002/2016PA003007

105. Yancey, T.E., and Liu, C., 2013. Impact-induced sediment deposition on an offshore, mud substrate continental shelf, Cretaceous/Paleogene boundary, Brazos River, Texas, USA. Journal of Sedimentary Research 83: 354-367.

106. Yonge, C.M., 1953. Form and habit in *Pinna carnea* Gmelin. Philosophical Transactions of the Royal Society of London, Series B. Biological Sciences 237. pp. 335-374.

107. Zhan, Q., Wang, Z., Xie, Y., Xie, J., He, Z., 2011. Assessing C/N and $\delta^{13}C$ as indicators of Holocene sea level and freshwater discharge changes in the subaqueous Yangtze delta, China. The Holocene, 697-704.

Tables

Table 1: Modes of life (Bush et al., 2007) exhibited by benthic molluscs in the grey unit of the Owl Creek Formation and spherule bed of the basal Clayton Formation, and proportional abundance in each unit. See Figure 9 for graphical representation of this data.

Number	Mode of life	Proportional abundance (grey unit)	Proportional abundance (spherule bed)
1	shallow infaunal, motile, carnivore	0.32	0.01
2	shallow infaunal, facultatively motile, unattached, suspension feeders	0.17	0.24
3	epifaunal, stationary, byssate, suspension feeders	0.17	0.02
4	deep infaunal, facultatively motile, suspension feeders	0.12	0
5	epifaunal, stationary, cemented, suspension feeders	0.06	0.18
6	epifaunal, motile, carnivores	0.06	0.13
7	epifaunal, facultatively motile, unattached, suspension feeders	0.03	0.17
8	semi-infaunal, stationary, byssate, suspension feeders	0.03	0
9	shallow infaunal, motile, surface deposit feeders	0.02	0.19
10	shallow infaunal, motile, suspension feeders	0.02	0.03
11	deep infaunal, facultatively motile, surface deposit feeders	0	0.01
12	epifaunal, facultatively motile, herbivores	0	0.01

Table 2: Index organic-walled dinoflagellate cysts from the 4th St. Quarry, AMNH 3481, Union Co., MS. See Figure 3 for location of samples relative to the lithostratigraphy.

Species	R6721F (7.5 cm)	R6721E (25 cm)	R6721D (40 cm)	R6721C (70 cm)
Cerodinium striatum/diebelii complex		x		
Deflandrea galeata (Lejeune-Carpentier 1942) Lentin & Williams 1973	x		x	
Disphaerogena carposphaeropsis Wetzel 1933	x	x		
Manumiella seelandica (Lange 1969) Bujak & Davies 1983		x		
Palynodinium grallator Gocht 1970	x	x	x	x
Piercites pentagonum (May 1980) Habib & Drugg 1987	x	x	x	

Highlights

- Describes new outcrops containing the Cretaceous–Paleogene (K–Pg) boundary from Union County, Mississippi.
- The fossiliferous Owl Creek Formation contains ammonites and diverse benthic molluscan fauna.
- Biostratigraphic correlation by macro and microfossils is consistent with deposition during the latest Maastrichtian.
- A 15–30 cm-thick event bed with macrofossils and impact spherules occurs above the K–Pg boundary.
- Spherule bed was emplaced rapidly by multiple processes following the Chicxulub impact event.